USGS
science for a changing world

National Water-Quality Assessment Program

Scaling Up Watershed Model Parameters—Flow and Load Simulations of the Edisto River Basin, South Carolina, 2007–09

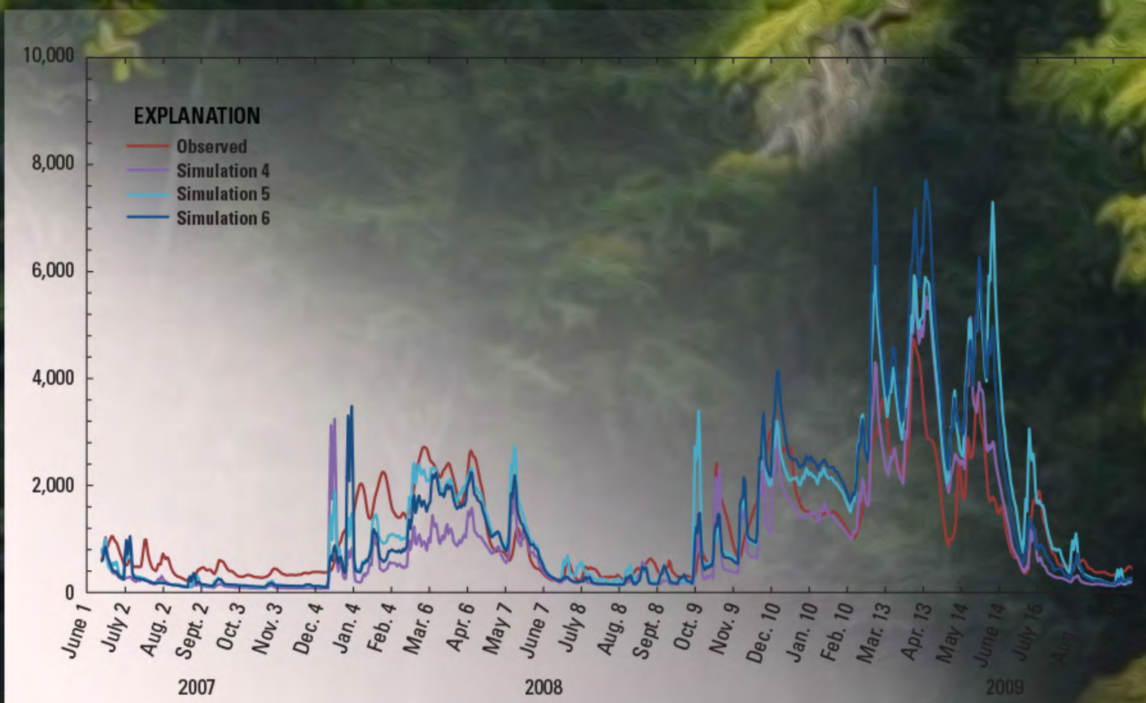

Scientific Investigations Report 2014–5104

U.S. Department of the Interior
U.S. Geological Survey

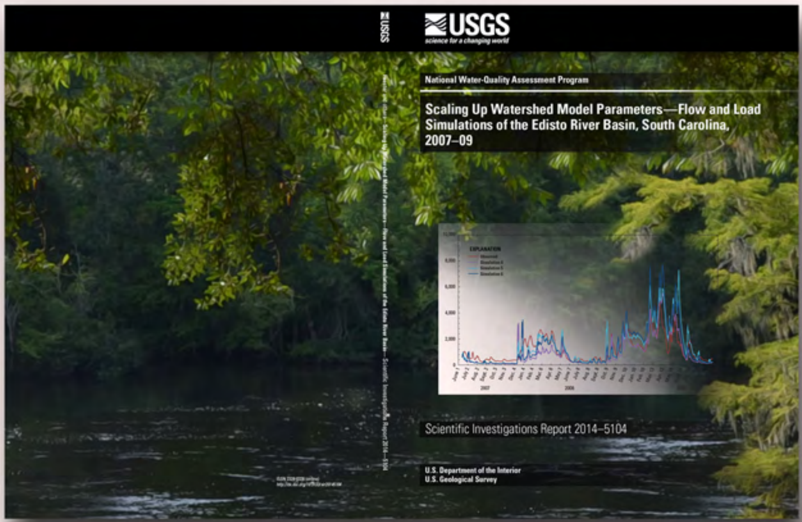

Cover: Edisto River in close proximity to the streamgage near Givhans at the State Highway 61 crossing, Dorchester County, South Carolina. Graph image from report figure 8*B*.

Scaling Up Watershed Model Parameters—Flow and Load Simulations of the Edisto River Basin, South Carolina, 2007–09

By Toby D. Feaster, Stephen T. Benedict, Jimmy M. Clark, Paul M. Bradley, and Paul A. Conrads

National Water-Quality Assessment Program

Scientific Investigations Report 2014–5104

U.S. Department of the Interior
U.S. Geological Survey

U.S. Department of the Interior
SALLY JEWELL, Secretary

U.S. Geological Survey
Suzette M. Kimball, Acting Director

U.S. Geological Survey, Reston, Virginia: 2014

For more information on the USGS—the Federal source for science about the Earth, its natural and living resources, natural hazards, and the environment, visit http://www.usgs.gov or call 1–888–ASK–USGS.

For an overview of USGS information products, including maps, imagery, and publications, visit http://www.usgs.gov/pubprod

To order this and other USGS information products, visit http://store.usgs.gov

Suggested citation:
Feaster, T.D., Benedict, S.T., Clark, J.M., Bradley, P.M., and Conrads, P.A., 2014, Scaling up watershed model parameters—Flow and load simulations of the Edisto River Basin, South Carolina, 2007-09: U.S. Geological Survey Scientific Investigations Report 2014–5104, 34 p., *http://dx.doi.org/10.3133/sir20145104.*

ISSN 2328-0328 (online)

Contents

Figures

Tables

Conversion Factors

Inch/Pound to SI

Multiply	By	To obtain
	Length	
inch (in.)	2.54	centimeter (cm)
inch (in.)	25.4	millimeter (mm)
	Area	
square mile (mi^2)	2.590	square kilometer (km^2)
	Flow rate	
cubic foot per second (ft^3/s)	0.02832	cubic meter per second (m^3/s)

SI to Inch/Pound

Multiply	By	To obtain
	Length	
meter (m)	3.281	foot (ft)
kilometer (km)	0.6214	mile (mi)
	Area	
hectare (ha)	2.471	acre
square kilometer (km^2)	247.1	acre
square kilometer (km^2)	0.3861	square mile (mi^2)
	Hydraulic conductivity	
meter per day (m/d)	3.281	foot per day (ft/d)

Temperature in degrees Celsius (°C) may be converted to degrees Fahrenheit (°F) as follows:

°F=(1.8×°C)+32

Temperature in degrees Fahrenheit (°F) may be converted to degrees Celsius (°C) as follows:

°C=(°F-32)/1.8

Vertical coordinate information is referenced to North American Vertical Datum of 1988 (NAVD 88).

Horizontal coordinate information is referenced to the North American Datum of 1983 (NAD 83).

Elevation, as used in this report, refers to distance above the vertical datum.

Abbreviations

ASCII	American Standard Code for Information Interchange
COOP	Cooperative
DEM	digital elevation model
DOC	dissolved organic carbon
FORTRAN	Formula Translating System
GBMM	grid-based mercury model
GHCN	Global Historical Climatology Network
GIS	geographic information system
HADS	Hydrometeorological Automated Data System
IDW	inverse distance weighting
m	scaling parameter
MAE	mean absolute error
MeHg	methylmercury
MPE	multisensory precipitation estimation
NAWQA	National Water-Quality Assessment Program
NCDC	National Climatic Data Center
NCEP	National Center for Environmental Prediction
NED	National Elevation Dataset
NEXRAD	next generation weather radar
ng/L	nanogram per liter
NHD	National Hydrography Dataset
NLCD	National Land-Cover Dataset
NOAA	National Oceanic and Atmospheric Administration
NSE	Nash-Sutcliffe coefficient of model-fit efficiency
NWS	National Weather Service
PBIAS	percent bias
PEST	parameter estimation program
r	(Pearson's) correlation coefficient
RMSE	root mean square error
SI	International System of Units
SSURGO	Soil Survey Geographic Database
subv	velocity to route water in channels
TOPLOAD	water-quality load model developed from TOPMODEL

TOPLOAD–H	water-quality load model developed from TOPMODEL with Hornberger's groundwater partitioning algorithm
TOPMODEL	topography-based hydrological model
TWI	topographic wetness index
USGS	U.S. Geological Survey
VELMA	Visualizing Ecosystems for Land Management Assessment model
WATER	Water Availability Tool for Environmental Resources
zroot	depth of root zone

Scaling Up Watershed Model Parameters—Flow and Load Simulations of the Edisto River Basin, South Carolina, 2007–09

By Toby D. Feaster, Stephen T. Benedict, Jimmy M. Clark, Paul M. Bradley, and Paul A. Conrads

Abstract

As part of an ongoing effort by the U.S. Geological Survey to expand the understanding of relations among hydrologic, geochemical, and ecological processes that affect fish-tissue mercury concentrations within the Edisto River Basin, analyses and simulations of the hydrology of the Edisto River Basin were made using the topography-based hydrological model (TOPMODEL). A primary focus of the investigation was to assess the potential for scaling up a previous application of TOPMODEL for the McTier Creek watershed, which is a small headwater catchment to the Edisto River Basin. Scaling up was done in a step-wise manner, beginning with applying the calibration parameters, meteorological data, and topographic-wetness-index data from the McTier Creek TOPMODEL to the Edisto River TOPMODEL. Additional changes were made for subsequent simulations, culminating in the best simulation, which included meteorological and topographic wetness index data from the Edisto River Basin and updated calibration parameters for some of the TOPMODEL calibration parameters. The scaling-up process resulted in nine simulations being made. Simulation 7 best matched the streamflows at station 02175000, Edisto River near Givhans, SC, which was the downstream limit for the TOPMODEL setup, and was obtained by adjusting the scaling factor, including streamflow routing, and using NEXRAD precipitation data for the Edisto River Basin. The Nash-Sutcliffe coefficient of model-fit efficiency and Pearson's correlation coefficient for simulation 7 were 0.78 and 0.89, respectively. Comparison of goodness-of-fit statistics between measured and simulated daily mean streamflow for the McTier Creek and Edisto River models showed that with calibration, the Edisto River TOPMODEL produced slightly better results than the McTier Creek model, despite the substantial difference in the drainage-area size at the outlet locations for the two models (30.7 and 2,725 square miles, respectively).

Along with the TOPMODEL hydrologic simulations, a visualization tool (the Edisto River Data Viewer) was developed to help assess trends and influencing variables in the stream ecosystem. Incorporated into the visualization tool were the water-quality load models TOPLOAD, TOPLOAD–H, and LOADEST. Because the focus of this investigation was on scaling up the models from McTier Creek, water-quality concentrations that were previously collected in the McTier Creek Basin were used in the water-quality load models.

Introduction

Methylmercury (MeHg) contamination is the leading cause of fish consumption advisories in the United States, affecting 40 percent of lake area and 36 percent of river distance (U.S. Environmental Protection Agency, 2011). Over 4,700 water bodies in the United States are reported on State Clean Water Act Section 303(d) lists as being impaired due to mercury (U.S. Environmental Protection Agency, 2013). Mercury-specific fish consumption advisories affect more than half of South Carolina, including the entire Coastal Plain physiographic province within the State. Methylmercury is the primary form of mercury in fish (Bloom, 1992). Exposure to methylmercury may cause immune system suppression, neurodevelopmental delays, and compromised cardiovascular health in humans (Mergler and others, 2007), as well as behavioral, neurochemical, hormonal, and reproductive changes in wildlife (Scheuhammer and others, 2007; 2012).

In the summer and fall of 1998, the National Water Quality Assessment (NAWQA) and Toxic Substances Hydrology (Toxics) Programs of the U.S. Geological Survey (USGS) conducted a national pilot survey of mercury concentrations in the sediment and water (Krabbenhoft and others, 1999) and in axial muscle tissues of top predator fish (Brumbaugh and others, 2001) from 107 sites in 20 stream basins across the United States. The results identified the Edisto River, a Coastal Plain stream in South Carolina, as having some of the highest top predator fish mercury concentrations in the Nation. A follow-up assessment demonstrated that the highest fish mercury concentrations not related to mining activities occurred in "black-water" (high dissolved organic carbon [DOC]) Coastal Plain streams in the eastern and southeastern United States (Bauch and others, 2009; Scudder and others, 2009). The follow-up assessment included the data from the original 107 sites in the pilot survey, 159 stream sites from a second USGS national survey conducted in 2002 and 2004–5, and 101 stream sites from four USGS regional studies conducted during 1998–2005 (Bauch and others, 2009; Scudder and others, 2009). Results from the follow-up assessment indicated that stream habitats within the Coastal Plain of the predominantly forested/agricultural southeastern United States were among the most vulnerable ecosystems to mercury in North America (Bauch and others, 2009; Brumbaugh and others, 2001; Krabbenhoft and others, 1999; Scudder and others, 2009). Despite the recognized pattern of elevated mercury concentrations in fish (Brumbaugh and others, 2001; Glover and others, 2010; Guentzel, 2009; Krabbenhoft and others, 1999; Scudder and others, 2009) in this geographically extensive physiographic region (Fenneman, 1928, 1938; Vigil and others, 2000), comparatively little is known about the fundamental controls on mercury bioaccumulation in the Coastal Plain of the southeastern United States. Thus, understanding the fundamental hydrologic, geochemical, and ecological processes that affect the levels of fish-tissue mercury concentrations within Coastal Plain streams like the Edisto River Basin is an environmental priority.

Fluvial networks are "open" systems (river continuum [Sedell and others, 1989; Vannote and others, 1980] and flood pulse [Junk and others, 1989] concepts) characterized by substantial changes in physical and ecological structure over order-of-magnitude ranges in spatial scales, (from headwaters to downstream estuarine/marine margins) (Thorp and others, 2006). Any upstream biogeochemical process theoretically may influence downstream aquatic food webs (Vannote and others, 1980), with the impact decreasing with downstream separation (Sedell and others, 1989). Understanding anthropogenic and environmental controls on fluvial mercury bioaccumulation in large basins can therefore be challenging because of the need to integrate over scales ranging from microscopic to regional. Thus, because comprehensive source-to-receptor investigations increase in difficulty with basin size (Bradley and others, 2011, 2010; Brigham and others, 2009; Chasar and others, 2009; Marvin-DiPasquale and others, 2009; Ward and others, 2010), coordinated investigations of multiple scales within individual basins are rare (Bradley and others, 2011; Brigham and others, 2009). Accordingly, the majority of efforts to better understand the biogeochemical drivers of stream mercury bioaccumulation within large basins, and across regional and national gradients, are typically conducted in small basins at scales of less than about 30 square miles (mi^2).

Pollutant management strategies are often implemented at broad spatial scales (State, regional, and national). Although research is often performed at reach to small-basin scales, regional and regulatory actions are taken at larger scales too extensive to fully characterize with limited time and resources. Scaling up is particularly important for mercury, because limited information is available at broader watershed and regional scales (Ali and others, 2013; Bradley and others, 2013; Clark and others, 2009; Sivapalan, 2003). Watershed models are essential for ecological risk management and potentially critical tools for addressing risk at multiple scales within large basins and across regions. Consequently, the scalability of small-basin study results is a fundamental issue in the development of models for large-basin and regional applications. The USGS is collaborating with the U.S. Environmental Protection Agency (EPA) to assess the potential for upscaling of multiple models developed in small basin settings for applications at broader watershed scales.

Wetlands are recognized source areas for environmental methylmercury (Bradley and others, 2010, 2011, 2012, 2013; Brigham and others, 2009; Grigal, 2002; St. Louis and others, 1994). Thus, the risk of mercury contamination in the Edisto River Basin aquatic environment, including the risk to human health, is inextricably linked to hydrologic transport of methylmercury from the site and matrix of production in the wetlands to aquatic habitats in the adjacent stream reach and farther downstream in the basin (Bradley and others, 2009; Chasar and others, 2009). A recent study (Bradley and others, 2010) demonstrated that the coarse-grained sediments that characterize much of the Coastal Plain support the efficient exchange of water between wetlands and stream habitats through continuous connectivity of groundwater discharge from the shallow subsurface toward the stream-channel habitat, even during flood conditions. This efficient exchange of water promotes the transport of methylmercury from riparian wetland source areas to the stream aquatic habitat and, consequently, makes Coastal Plain streams inherently vulnerable to mercury bioaccumulation. Stream systems, such as the Edisto River, that are entirely or largely within the Coastal Plain are particularly vulnerable to mercury bioaccumulation.

In light of the critical role of hydrology as a driver of methylmercury concentrations within the stream aquatic habitats of the Edisto River Basin in particular and the Coastal Plain in general, numerical tools that reliably simulate the direction, timing, and quantity of water transport contribute substantially to better understanding and management of mercury risk across multiple scales. Previous reports describe the development and application of a hydrologic model (TOPMODEL) for McTier Creek (Feaster and others, 2010, 2012), a small headwater catchment that covers about 38 mi^2 of the Edisto River Basin. A recent intra-basin mercury assessment conducted in the Edisto River Basin of South Carolina suggests that results from small basin studies provide a reasonable foundation for development of orders-of-magnitude upscaled conceptual or numerical models for application at large-basin and regional scales within the Edisto River Basin and within the Coastal Plain (Bradley and others, 2013).

Building upon the application of TOPMODEL to McTier Creek (Feaster and others, 2010, 2012), which is a small headwater catchment of the Edisto River Basin, a primary purpose of this investigation was to scale up TOPMODEL to the larger Edisto River Basin. Hydrologic simulations from TOPMODEL were then applied to TOPLOAD and TOPLOAD–H to evaluate water-quality loads associated with water-quality constituents such as mercury. Similar to the McTier Creek watershed investigation (Benedict and others, 2012; Feaster and others, 2010; Golden and others, 2012), the hydrologic and water-quality output from this simulation will be used to provide a framework for an improved understanding of the spatial and temporal variability relation of mercury and hydrology in the larger Coastal Plain basin. The development of multi-scale hydrologic and associated mercury biogeochemistry model frameworks for the Edisto River basin directly addresses the strategic goals of the USGS to understand ecosystems and predict ecosystem change as well as provide the Nation with the information needed to meet the challenges of the 21st century (U.S. Geological Survey, 2007).

Purpose and Scope

The purpose of this report is to present analyses and simulations of the flows and selected water-quality loads of the Edisto River Basin using the topography-based hydrological model (TOPMODEL; Beven and Kirkby, 1979), and TOPLOAD and TOPLOAD–H (Benedict and others, 2012), which are water-quality load models that use output from the TOPMODEL. Specifically, this report assesses the potential for upscaling the McTier Creek TOPMODEL to the larger Edisto River Basin (about 2,730 mi^2). Following a brief characterization of TOPMODEL, the report documents the data and other information used as model input. The step-wise application of TOPMODEL to the Edisto River through various simulations is then documented in terms of the parameters and input data used in each case. Selected goodness-of-fit statistics as well as single-mass curves and flow duration curves are used to characterize simulation results. Lastly, the Edisto River Data Viewer is described, with emphasis on the water-quality load models incorporated in this utility.

U.S. Geological Survey streamflow data are measured and reported in English units; consequently, most of the data presented in this report are provided using English units. However, because the models used in this investigation include both English and International System of Units (SI), the report includes both systems of measurement.

Previous TOPMODEL Studies

TOPMODEL is a physically based watershed model that simulates the variable-source-area concept of streamflow generation (Wolock, 1993). The model was first described by Beven and Kirkby (1979) and has continually evolved along with the understanding of how precipitation moves over and through watersheds and ultimately contributes to streamflow. By design, the modeling concepts in TOPMODEL have been kept simple to preserve a flexible model structure that can be tailored based on the researcher's perceptions of the behavior of a particular watershed (Singh, 1995). As a result, numerous versions of TOPMODEL exist. Beven (1997) documents a variety of versions and applications of TOPMODEL.

The version of TOPMODEL used in this investigation was first documented by Kennen and others (2008) and subsequently by Feaster and others (2010), as applied in the McTier Creek watershed in South Carolina. In the McTier Creek watershed, TOPMODEL was utilized to provide a framework for improved understanding of the spatial and temporal variability of the relation between hydrology and mercury transport (Golden and others, 2012). As part of a contrasting investigation to the McTier Creek study, TOPMODEL was applied to the Fishing Brook watershed, New York (Journey and others, 2012; Nystrom and Burns, 2011). Fishing Brook is a tributary to the Hudson River near its headwaters, is located in the Adirondacks of upstate New York, and is mostly forested with little impervious surface.

In a follow-up investigation to the McTier Creek study, the model from McTier Creek was used to compare TOPMODEL streamflow simulations by using measured rainfall data, as was done in the investigation by Feaster and others (2010), with simulations generated using next generation weather radar (NEXRAD) rainfall data (Feaster and others, 2012). During that investigation, a single sign error in the TOPMODEL source code that caused an error in the intra-time-step water-balance calculations was discovered and corrected. Comparison simulations showed that the influence on the streamflow simulations from TOPMODEL was minor (Feaster and others, 2012). In addition, measured rainfall data from six National Weather Service (NWS) Cooperative (COOP) stations surrounding the McTier Creek watershed that were used to calibrate the McTier Creek TOPMODEL were compared to NEXRAD rainfall data generated at the NWS COOP stations. Based on separate calibrations, the goodness-of-fit statistics indicated similar results for TOPMODEL streamflow simulations using the NWS COOP data and those using the NEXRAD data.

As part of an investigation to model ungaged streams in Kentucky, Williamson and others (2009) incorporated the TOPMODEL documented by Kennen and others (2008) into the Water Availability Tool for Environmental Resources (WATER). In the investigation by Kennen and others (2008), TOPMODEL was part of an integrated hydroecological model that provided a comprehensive set of hydrologic variables representing major components of the flow regimes at 856 aquatic-invertebrate monitoring sites in New Jersey. Kennen and others (2008) noted that the TOPMODEL code used in their study had been modified from an earlier version used in an investigation by Wolock (1993). The purpose of the Wolock (1993) report was to describe the theoretical background of TOPMODEL, the model equations, the methods used to determine parameter values, and the FORTRAN computer code. The report also provides an extensive list of papers and reports for which TOPMODEL has been used to study a variety of research areas.

Wolock (1993) stated that the version of TOPMODEL described therein was derived from the version documented by Hornberger and others (1985), with extensive modifications. Hornberger and others (1985) modified the version of TOPMODEL documented by Beven and Wood (1983) and applied it to a small, forested catchment in Shenandoah National Park, Virginia.

As part of the previous investigation of McTier Creek, Benedict and others (2012) developed the TOPLOAD and TOPLOAD–H load models that apply a mass-balance algorithm to the surface and subsurface flows simulated by the TOPMODEL, providing a means to assess the surface and subsurface mass fluxes for a given water-quality constituent. The TOPLOAD model uses the surface and subsurface flow components directly from TOPMODEL, computing a load for each flow component. TOPLOAD–H, a variant of TOPLOAD, modifies the subsurface hydrologic components of TOPMODEL by using the groundwater-partitioning algorithm presented in Hornberger and others (1994). The TOPLOAD and TOPLOAD–H models were used to enable comparisons with other mercury load models (Golden and others, 2012) and to compare projections of future watershed mercury-load export under different climate-change scenarios (Golden and others, 2013).

Description of the Edisto River Basin

The Edisto River is the longest and largest river system completely contained in South Carolina and is one of the longest free-flowing black-water rivers in the United States (South Carolina Department of Natural Resources, 2009). The basin is located in south-central South Carolina and includes parts of the upper and lower Coastal Plain regions (fig. 1; Marshall, 1993; South Carolina Department of Health and Environmental Control, 2012). The total basin encompasses about 3,150 mi^2 and is drained by four major rivers: North Fork Edisto River, South Fork Edisto River, Edisto River (main stem), and Four Hole Swamp.

The average yearly rainfall for the Edisto River Basin was 48.5 inches (in.) from 1971 to 2000 (South Carolina Department of Health and Environmental Control, 2012). The seasonal rainfall during this period ranged from a maximum of 15.75 in. during the summer to a minimum of 9.88 in. during the fall. The average annual daily temperature was 63.9 degrees Fahrenheit (°F), with the summer temperature averaging 79.4 °F and the winter temperature averaging 47.8 °F.

Streamflow in the Edisto River is fairly consistent and well sustained, largely because of groundwater reserves in the upper region of the Coastal Plain (South Carolina Department of Natural Resources, 2009). The focus of this investigation is the portion of the Edisto River Basin as monitored by USGS streamflow-gaging station 02175000, Edisto River near Givhans, SC (fig. 1). The published drainage area for station 02175000 is 2,730 mi^2 (U.S. Geological Survey, 2012). The USGS has monitored daily mean flow at station 02175000 since January 1939. Through September 2012, the annual mean flow at station 02175000 was 2,440 cubic feet per second (ft^3/s). The highest daily mean flow was 24,100 ft^3/s and was recorded on June 14, 1973. The lowest daily mean flow was 150 ft^3/s and was recorded on August 17, 2002.

TOPMODEL

The topography-based hydrological model (TOPMODEL) is a physically based watershed model that simulates streamflow by using the variable source-area concept of streamflow generation (fig. 2; Beven and Kirby, 1979; Hornberger and others, 1998). TOPMODEL is a semidistributed model that uses a topographic wetness index (TWI) to group hydrologically similar areas of a watershed. In the variable source-area concept, saturated land-surface areas are sources of streamflow during precipitation events in several ways. Saturation overland flow (also called Dunne overland flow) is generated if the subsurface is not transmissive and if slopes are gentle and convergent (Dunne and Black, 1970; Wolock, 1993). Saturation overland flow can arise from direct precipitation on the saturated land-surface areas or from return flow of subsurface water to the surface in the saturated areas. Subsurface storm flow is generated if the near-surface soil zone is very transmissive, having large saturated hydraulic conductivity, and if gravitational gradients (slopes) are steep. Whipkey (1965) defined subsurface storm flow as underground storm flow that reaches the stream channel without entering the groundwater storage zone.

In-depth discussions of the mathematical underpinnings of TOPMODEL are provided in Beven and Kirkby (1979), Beven (1997), Hornberger and others (1998), Wolock (1993), and Beven (2001). Feaster and others (2010, 2012) describe the calibration of TOPMODEL for the McTier Creek watershed in considerable detail.

Observed Data Used for TOPMODEL Simulations

Hydrologic simulations in TOPMODEL require the following types of inputs: (1) a time series of meteorological data, (2) the TWI distribution, and (3) model parameters, including measured watershed characteristics and calibrated parameters. Streamflow data are not required for the model simulation but are used to assess how well the simulations capture the characteristics of the measured streamflow data.

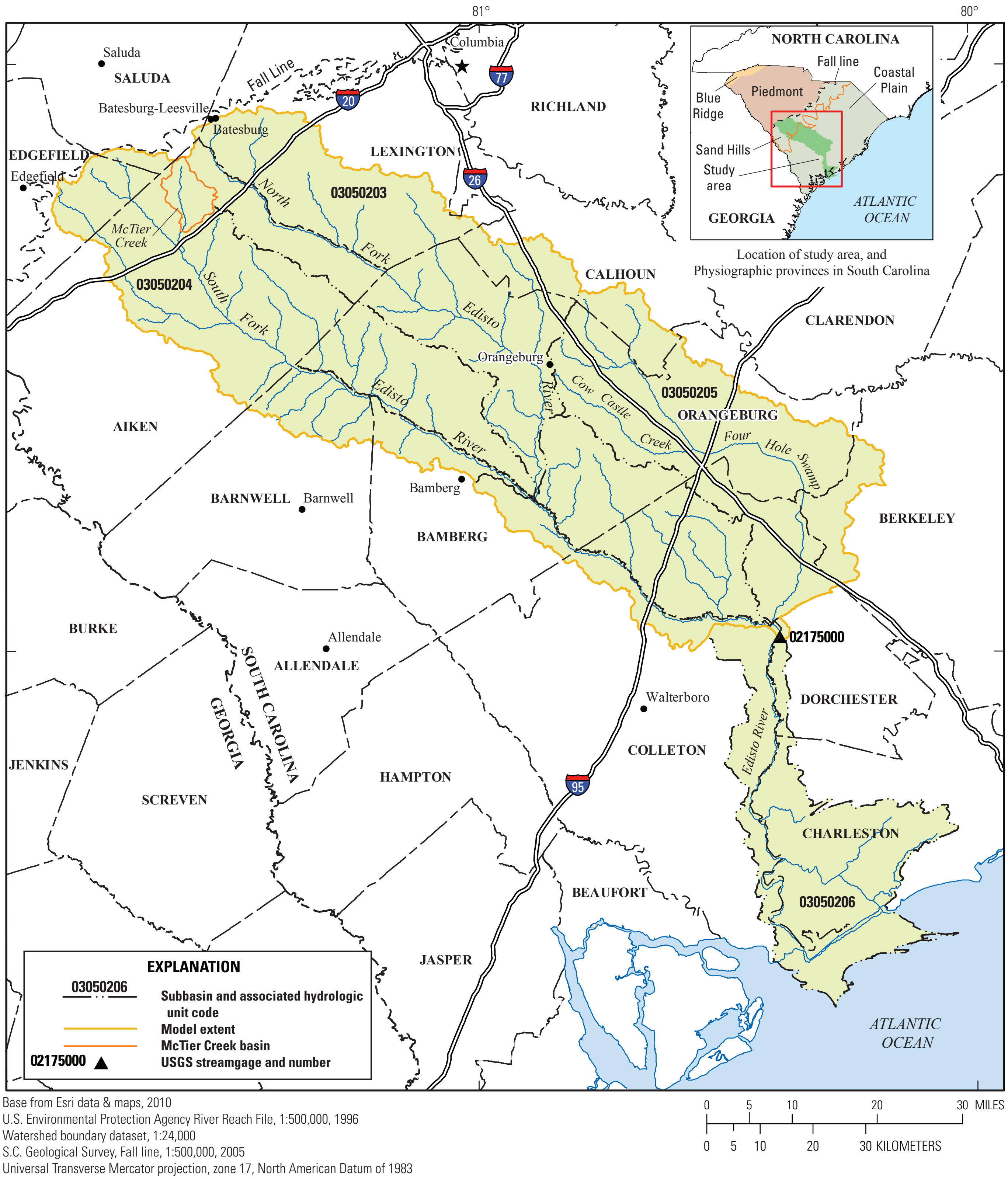

Figure 1. Edisto River Basin and U.S. Geological Survey station 02175000, Edisto River near Givhans, SC. [USGS, U.S. Geological Survey]

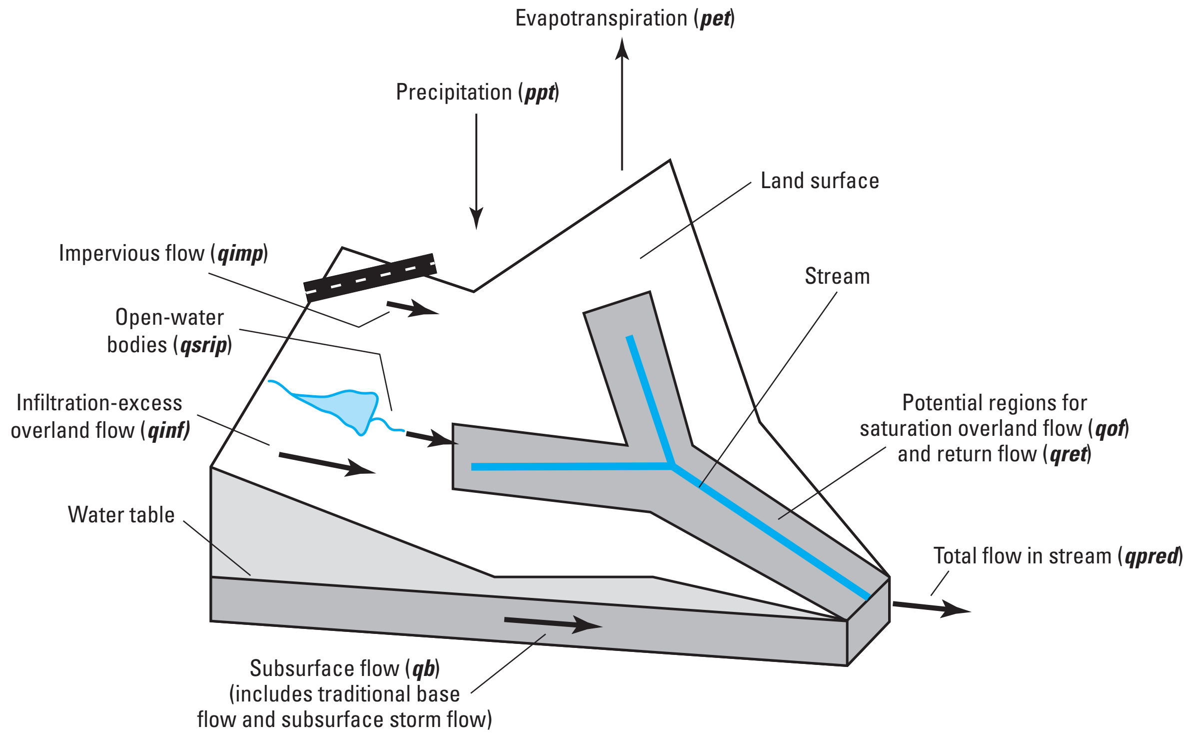

Figure 2. Definitions of selected water-source variables from TOPMODEL (modified from Wolock, 1993).

Precipitation and Air Temperature

The meteorological data required for the watershed modeling are daily precipitation and average daily air temperature. For an initial simulation, the meteorological data used in the McTier Creek TOPMODEL (Feaster and others, 2010) were used for the Edisto River model. Those data were obtained from the NWS COOP stations located in and around the McTier Creek watershed and were weighted using inversed distance weighting (IDW) based on the distance from each NWS station to the centroid of the McTier Creek Basin. To better represent the meteorological characteristics of the larger Edisto River Basin, two additional sources of data also were compiled: NEXRAD stage IV precipitation data and Global Historical Climatology Network (GHCN) precipitation and air temperature data. The NWS COOP station data used in the McTier Creek investigation are part of the GHCN and consequently will hereafter be referred to as GHCN data.

Next-Generation Radar (NEXRAD) Stage IV Data

Daily gridded NEXRAD stage IV, or multisensory precipitation estimation (MPE), data for 2006–9 were obtained from the National Oceanic and Atmospheric Administration (NOAA) National Center for Environmental Prediction (NCEP). The TOPMODEL simulations were run for the period from June 13, 2007, to September 30, 2009, which was concurrent with the period simulated for McTier Creek (Feaster and others, 2010, 2012). TOPMODEL uses 1 year of meteorological data as a warm-up period, so the simulations actually began on June 13, 2006. Stage IV data are adjusted using Hydrometeorological Automated Data System (HADS) precipitation data (National Weather Service, 2013). Data were extracted as GIS point shapefiles using the NOAA’s Weather and Climate Toolkit (National Oceanic and Atmospheric Administration, 2013). The points represent an approximate 4-km by 4-km grid. Shapefiles were clipped to the study area and averaged for each day using batch processing.

Global Historical Climatology Network Data

Meteorological data from the National Climatic Data Center (NCDC) were assessed using a daily time step. From that review, NCDC meteorological data that are part of the GHCN were compiled from 21 stations in or around the Edisto River Basin (fig. 3; table 1; Menne and others, 2012). Records for most GHCN stations had some days for which data were missing. For the Springfield station, precipitation data were available for less than 80 percent of the period analyzed; therefore, the station was excluded from the weighting analysis. For all the other stations, the precipitation data were available for 91 to 100 percent of the period analyzed.

The meteorological data were reviewed and compared using single-mass curves, which present a cumulative plot of data over time and represent the volume of the parameter being reviewed. The single-mass curves were generated using

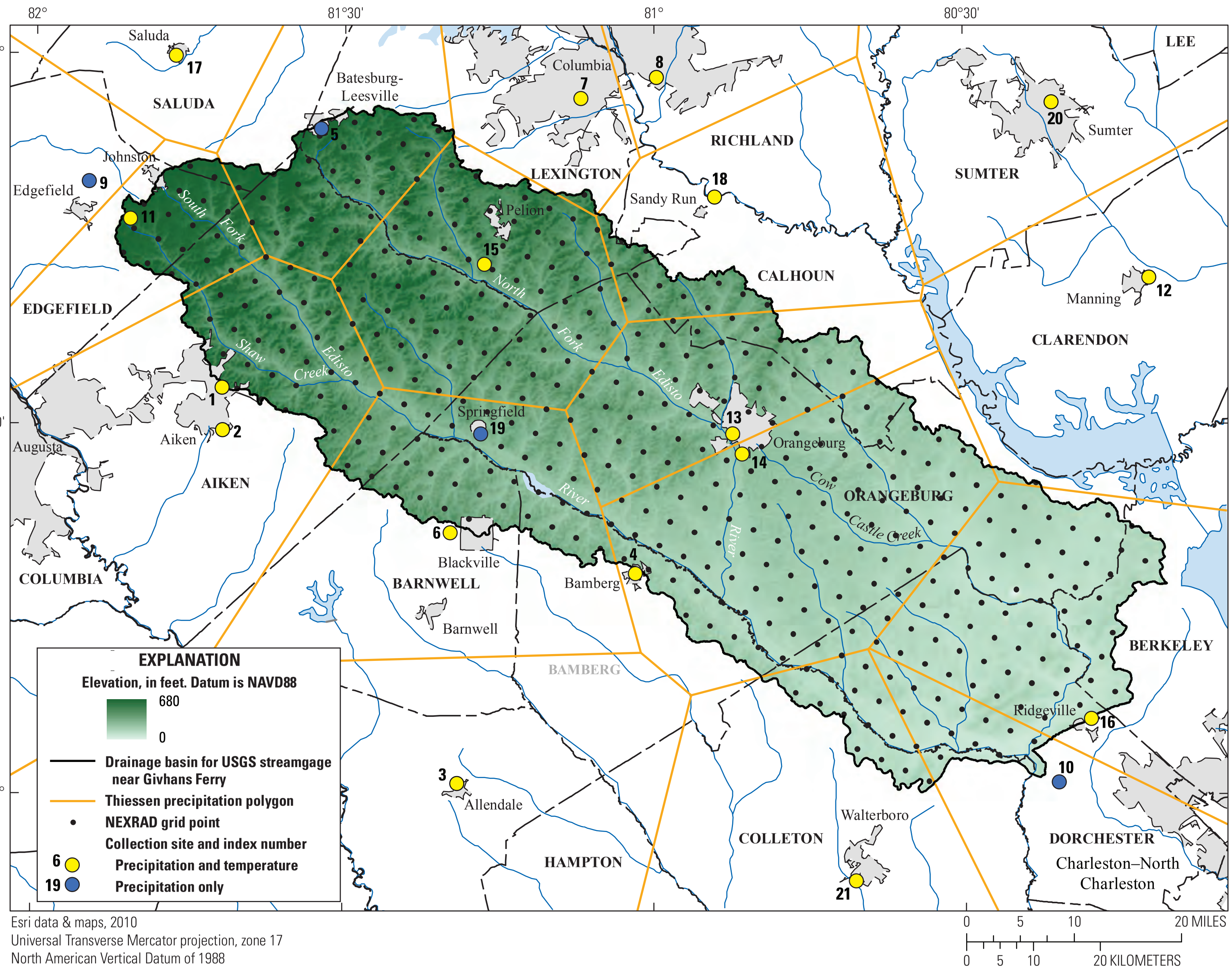

Figure 3. Meteorological stations in the vicinity of the Edisto River Basin, South Carolina, considered for use in this investigation. [NEXRAD, Next generation weather radar; USGS, U.S. Geological Survey]

Table 1. Meteorological stations in and around the Edisto River basin, South Carolina, considered for use in this investigation.

Map index number (fig. 3)	Station name	Station identifier	Latitude	Longitude	Parameters available	Distance to centroid of Edisto River Basin (miles)
1	Aiken 2 E	GHCND:USC00380072	33°33'00.00"N	81°41'48.01"W	Rainfall, temperature	39.7
2	Aiken 5 SE	GHCND:USC00380074	33°29'33.00"N	81°41'44.99"W	Rainfall, temperature	39.7
3	Allendale 2 NW	GHCND:USC00380126	33°00'57.60"N	81°18'57.60"W	Rainfall, temperature	37.1
4	Bamberg	GHCND:USC00380448	33°18'00.00"N	81°01'48.00"W	Rainfall, temperature	12.9
5	Batesburg	GHCND:USC00380506	33°54'00.00"N	81°32'20.00"W	Rainfall	42.0
6	Blackville 3W	GHCND:USW00063826	33°21'18.00"N	81°19'40.44"W	Rainfall, temperature	20.6
7	Columbia Metropolitan Airport	GHCND:USW00013883	33°56'30.84"N	81°07'05.16"W	Rainfall, temperature	32.5
8	Columbia Owens Downtown Airport	GHCND:USW00053867	33°58'14.02"N	80°59'44.99"W	Rainfall, temperature	33.7
9	Edgefield 3 NNE	GHCND:USC00382712	33°49'39.00"N	81°54'51.01"W	Rainfall	57.2
10	Givhans Ferry 2 ESE	GHCND:USC00383525	33°01'00.01"N	80°21'00.00"W	Rainfall	49.8
11	Johnston 4 SW	GHCND:USC00384607	33°46'39.00"N	81°50'48.01"W	Rainfall, temperature	52.2
12	Manning	GHCND:USC00385493	33°41'52.80"N	80°12'00.00"W	Rainfall, temperature	48.5
13	Orangeburg 2	GHCND:USC00386527	33°29'19.00"N	80°52'23.99"W	Rainfall, temperature	7.6
14	Orangeburg Municipal Airport	GHCND:USW00053854	33°27'42.01"N	80°51'29.02"W	Rainfall, temperature	8.6
15	Pelion 4 NW	GHCND:USC00386775	33°43'03.00"N	81°16'27.01"W	Rainfall, temperature	22.3
16	Ridgeville	GHCND:USC00387288	33°06'09.00"N	80°17'52.01"W	Rainfall, temperature	48.6
17	Saluda	GHCND:USC00387631	33°59'52.01"N	81°46'28.99"W	Rainfall, temperature	56.6
18	Sandy Run 3ENE	GHCND:USC00387683	33°48'32.04"N	80°54'06.84"W	Rainfall, temperature	23.3
19	Springfield	GHCND:USC00388219	33°29'35.02"N	81°16'46.99"W	Rainfall	15.7
20	Sumter	GHCND:USC00388440	33°56'09.60"N	80°21'21.60"W	Rainfall, temperature	48.6
21	Walterboro 1 SW	GHCDN:USC00388922	32°53'04.92"N	80°40'33.96"W	Rainfall, temperature	45.8

concurrent data from June 13, 2006, to September 30, 2009 (fig. 4). Differences in the volumes for the various stations can indicate the natural variability in rainfall over large areas; however, a significant deviation in the slope or pattern of a particular curve could indicate a problem with data. When the curves become horizontal, they indicate a period of missing data or a sustained period of no precipitation. For example, there was a break in the record for the Aiken station from November 1, 2008 to March 30, 2009, during the period after data collection had ended at Aiken 5SE and before data collection began at Aiken 2E. (Because of the close proximity of the two stations, the data at Aiken 5SE and Aiken 2E were combined for this investigation.) Consequently, that period of record was removed from all stations to facilitate comparison of concurrent data (fig. 4). As shown in figure 4, the Bamberg station data deviate significantly from the rest of the data for most of the period being compared. Consequently, the precipitation data from the Bamberg station were not included in the weighting analysis. The single-mass curves with the Aiken and Bamberg stations excluded (fig. 5) have similar shapes and slopes, and again highlight the natural variability in rainfall data in and around the Edisto River Basin. For the concurrent period that was analyzed, the total rainfall volume ranged from 51.4 in. at Columbia Owens Downtown Airport to 76.8 in. at Givhans Ferry 2 ESE (fig. 4).

Minimum and maximum air temperature data were obtained from the GHCN and then used to compute a daily average temperature for each day. Single-mass curves also were used to review the concurrent average daily air temperature for the period from June 13, 2006, to September 30, 2009 (fig. 6). As would be expected with air temperature, the curves show very little variability across the region. The analysis indicated no problems with the air temperature data from any of the GHCN stations reviewed and, therefore, all the stations were included in the weighting analysis.

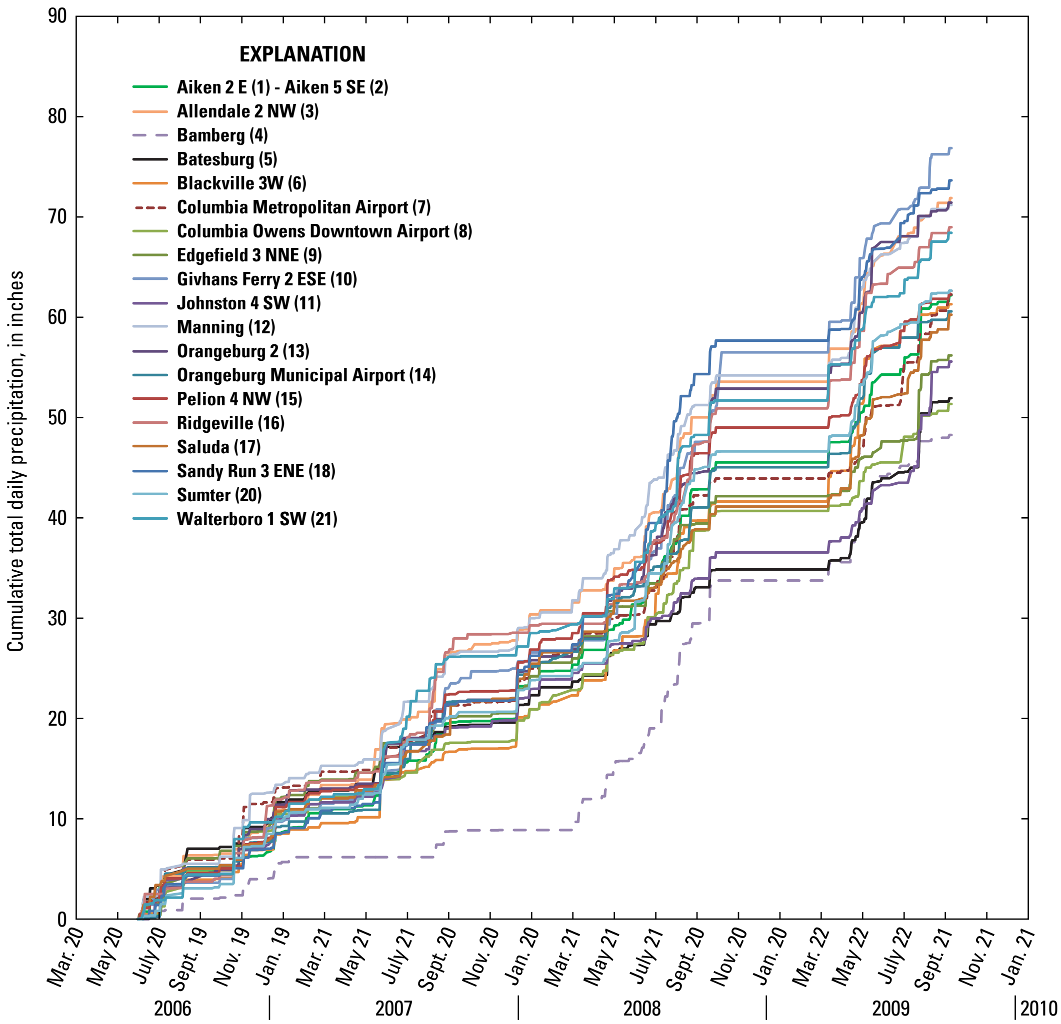

Figure 4. Single-mass curves of precipitation data from the Global Historical Climatology Network Data (map index number from table 1 shown in parenthesis).

Inverse Distance Weighting of Global Historical Climatology Network Data

As was done for the McTier Creek meteorological data (Feaster and others, 2010), the GHCN precipitation and average air temperature data were weighted by using IDW. The weighting for the Edisto River Basin meteorological data was based on the distance from each GHCN station to the centroid of the Edisto River Basin.

$$Z_k = \frac{\sum_{i=1}^{n} \frac{Z_i}{d_i^2}}{\sum_{i=1}^{n} \frac{1}{d_i^2}} \quad (1)$$

where

Z_k is the weighted meteorological value at the centroid of Edisto River Basin;

Z_i is the meteorological value at the GHCN station; and

d_i is the distance from the centroid of the watershed to the GHCN station (in miles).

After initial TOPMODEL simulations, there was concern that the IDW procedure might not accurately capture rainfall when it is highly variable across the watershed because IDW gives the most weight to stations closest to the basin centroid. This is a potential issue for the Edisto River Basin and others that are comparably large and elongated in shape, because there could be periods when rainfall is heavy in the upper or lower part of the basin but not in the middle part. Using the IDW method for such instances, the stations nearest to the centroid would still receive the most weight. A second weighting method (Thiessen) was used in order to address this potential issue.

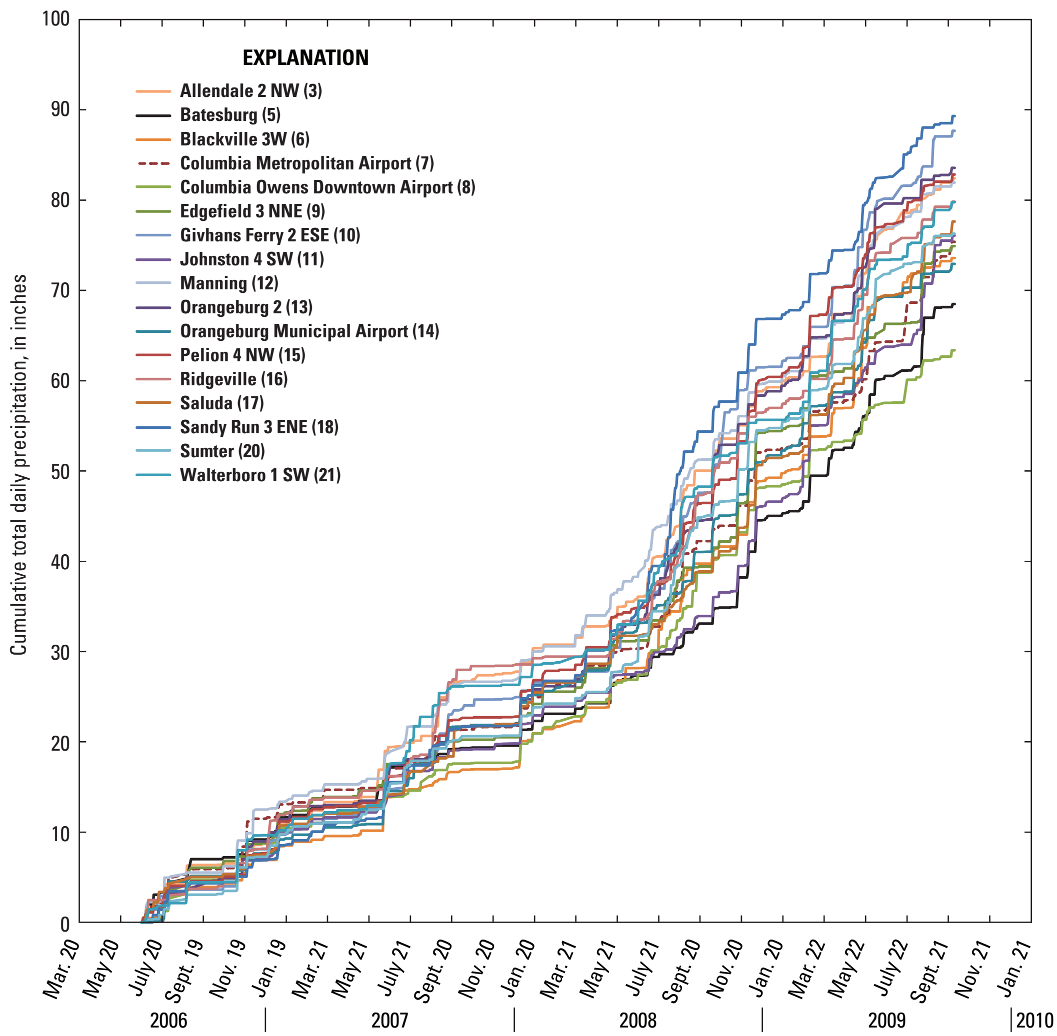

Figure 5. Single-mass curves of precipitation data from the Global Historical Climatology Network Data excluding Bamberg and Aiken 2 S (5 SE) (map index number from table 1 shown in parenthesis).

Thiessen Polygon Weighting of Global Historical Climatology Network Data

The Thiessen polygon method involves areal weighting (Bedient and others, 2008) and thus for a large, elongated basin it could possibly provide a better representative weighted value than IDW. The Thiessen method creates a polygon for each selected station with regard to its position relative to other stations so that any location within a polygon is closest to that polygon's station (fig. 3; Esri, 2013). Precipitation and air temperature are considered uniform within each polygon. The "create Thiessen polygons" tool in ArcGIS was used to determine the polygons, which were then clipped to the study basin boundary and the area for each polygon calculated. The calculation to determine the daily average value is as follows:

$$\text{Average precipitation (or temperature)} = (x_1{*}p_1) + (x_2{*}p_2) + \ldots + (x_i{*}p_i) \,/\, (x_1+x_2+\ldots+x_i) \qquad (2)$$

where

x_i is the area of the *i*th individual polygon, and
p_i is the precipitation (or temperature) value for the *i*th individual polygon.

If a station had missing data on a given day, the weighting formula was adjusted so as to exclude that station for that day.

For the simulation period from June 13, 2006, to September 30, 2009, the precipitation data for the Edisto River Basin from the various sources were compared to the precipitation data from the McTier Creek investigation by using single-mass curves (fig. 7*A*; Feaster and others, 2010, 2012). Overall, the Thiessen and IDW weighted GHCN curves tend to be similar, with the Thiessen weighted method providing a slightly larger volume of rainfall. In addition, although the overall slopes of the curves were similar, the total volume of observed rainfall was slightly larger for the Edisto River Basin than for the McTier Creek Basin. As was the case for McTier Creek, the

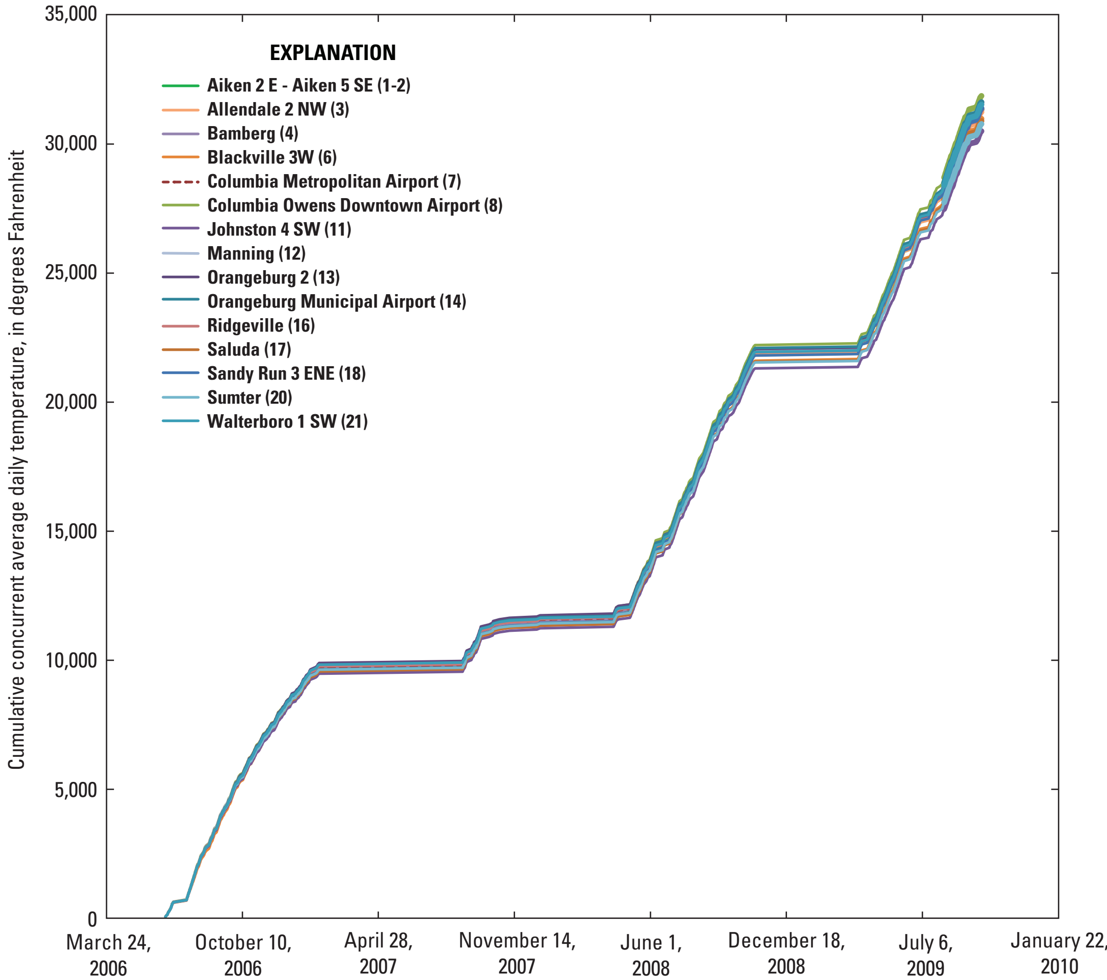

Figure 6. Single-mass curves of average daily air temperature from the Global Historical Climatology Network Data.

cumulative total daily NEXRAD precipitation data were lower than the observed precipitation data. Nonetheless, when the McTier Creek TOPMODEL was calibrated with the NEXRAD precipitation data, the goodness-of-fit statistics indicated results comparable to those obtained from a calibration using the observed rainfall data (Feaster and others, 2012).

A similar comparison of the average air temperature data also was made (fig. 7*B*). There was no substantial difference between the IDW and Thiessen-weighted temperature data. Air temperatures for the McTier Creek Basin were similar to those for the Edisto River Basin, although slightly lower overall.

Watershed Characteristics

In addition to the precipitation and air temperature data, other TOPMODEL inputs included watershed characteristics describing the topographic features, soil characteristics, and watershed latitude. Eight-digit hydrologic units for Four Hole Swamp, Edisto River, North Fork Edisto River, and the South Fork Edisto River were used to delineate the watershed boundary beginning at USGS station 02175000, (Eidson and others, 2005). It should be noted that the published drainage area for station 02175000 is 2,730 mi^2 (U.S. Geological Survey, 2012), which differs by less than 0.2 percent from the GIS drainage area of 7,058 square kilometers (km^2), or 2,725 mi^2, used in the TOPMODEL simulations. The drainage areas published in the annual USGS Water-Data Reports are rounded to three significant digits, which could account for the difference in the published drainage area for station 02175000 and the value computed in this investigation. To be consistent with the drainage area used in the computation of other weighted watershed characteristics generated for this investigation, however, the drainage area used in the TOPMODEL simulations was not rounded. Surface-water features were delineated using the 1:24,000-scale National Hydrography

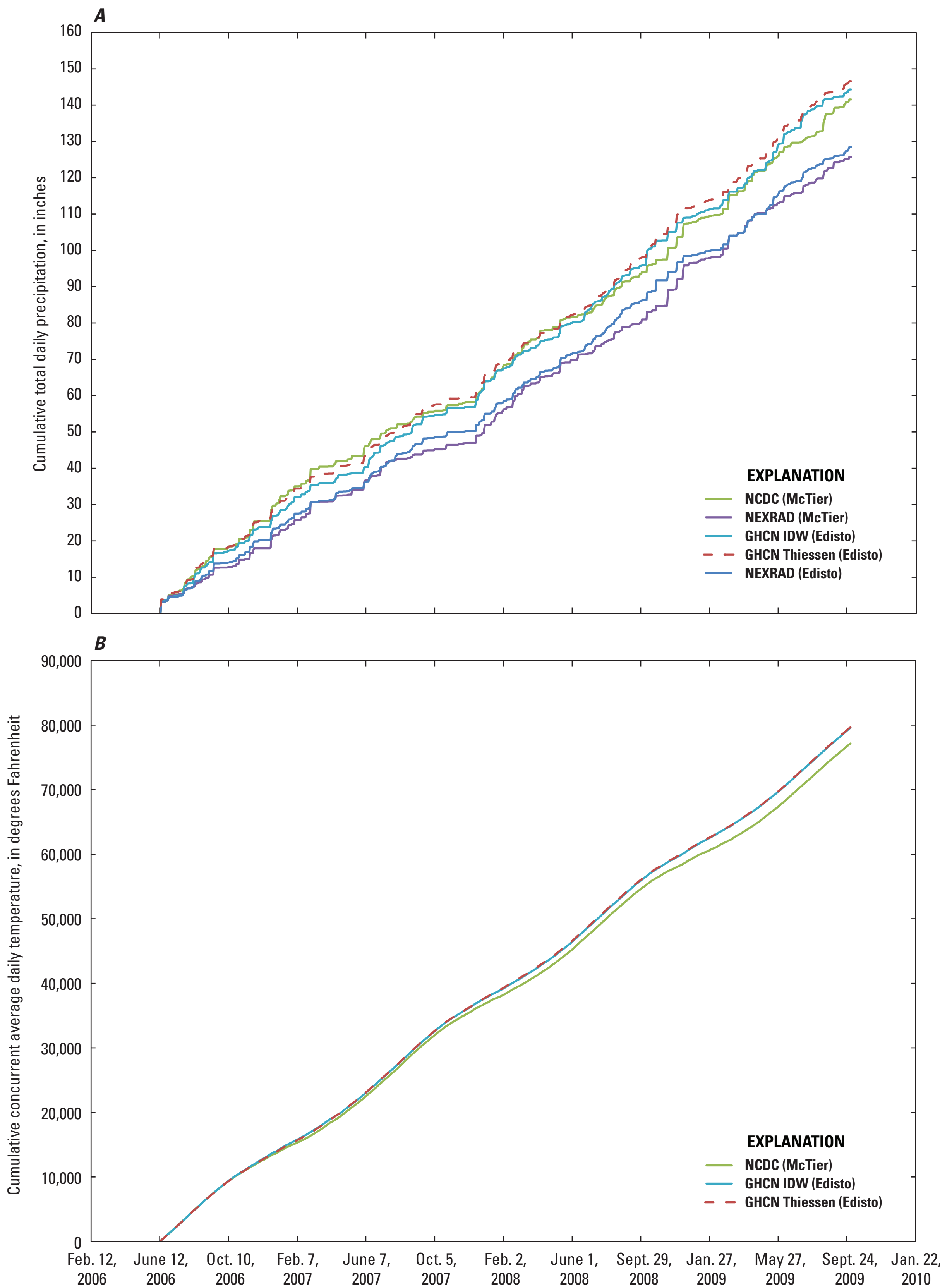

Figure 7. Single-mass curves for (*A*) the total daily precipitation and (*B*) average daily temperature for the McTier Creek and Edisto River Basins. [GHCN, Global Historical Climatology Network; IDW, inverse distance weighting; NEXRAD, Next generation weather radar; NCDC, National Climatic Data Center]

Dataset (NHD, 9.2 version 2.1). Impervious surface area was determined using a 30-meter grid of percent-developed imperviousness from the 2006 National Land-Cover Dataset (NLCD) (Fry and others, 2011).

Soil characteristics were determined using data from the Soil Survey Geographic (SSURGO) Database (Natural Resources Conservation Service, 2008). After the SSURGO data were preprocessed (Michael E. Wieczorek, U.S. Geological Survey, written commun., December 2008), the watershed model soil parameters were computed in ArcGIS using the zonal statistics tool and Soil Data Viewer (Natural Resources Conservation Service, 2013). Both vertical and horizontal data were weighted to determine average watershed values. The names, units of measure, and data sources for the measured watershed characteristics used in TOPMODEL are listed in table 2.

Topographic Wetness Index

The TWI is defined as

$$\mathrm{TWI} = \ln\,(a/\tan\,\beta) \tag{3}$$

where

TWI is the topographic wetness index, in ln (meters);
ln is the natural logarithm;
a is the upslope contributing area per unit contour length, in meters, and
tan β is the local slope, in degrees.

The TWI is used to describe how water accumulates in a drainage basin, based on a digital elevation model (DEM)

Table 2. Watershed characteristics for use with TOPMODEL.

[SSURGO, Soil Survey Geographic Database; TR–55, Technical Release 55]

Watershed characteristic	Unit	Data source
Total area	Square kilometer	1:24,000 digital raster graphics (*http://topomaps.usgs.gov/drg/*)
Lake area	Square kilometer	1:24,000-scale national hydrography dataset (*http://nhd.usgs.gov/*)
Stream area	Square kilometer	1:24,000-scale national hydrography dataset
Saturated conductivity	Inch per hour	SSURGO (*http://websoilsurvey.sc.egov.usda.gov/*) SSURGO
Soil depth	Inch	(calibration)
Field capacity	Unitless	SSURGO
Water holding capacity	Unitless	SSURGO
Porosity	Unitless	SSURGO
Percent impervious	Percent	National Land-Cover Dataset 2006 (*http://www.mrlc.gov/nlcd.php*)
Percent road impervious	Percent	National Land-Cover Dataset 2006 and National Map transportation layer (*http://nationalmap.gov/*)
Latitude	Decimal degrees	1:24,000 digital raster graphics
Uplake area	Square kilometer	1:24,000 digital raster graphics and 1:24,000-scale national hydrography dataset
Effective impervious	Decimal percent	Calibration
Percent macropore	Decimal percent	Calibration
Scaling parameter (m)	Inch	Calibration
subv (velocity to route water in channels)	Kilometer per day	Calibration
Depth of root zone (zroot)	Meter	Calibration
Impervious runoff constant	Unitless	Kennen and others (2008)
TR–55 curve number	Unitless	Kennen and others (2008)
Lake delay	Unitless	Calibration

(Quinn and others, 1997). High TWI values indicate areas having large contributing areas and relatively flat slopes, which typically are found at the base of hillslopes and near streams (large *a* value and small tan β value). These areas tend to be located where groundwater discharge would be expected to occur. Low TWI values tend to be found at the tops of hills where there is relatively little upslope contributing area and slopes are steep (small *a* value and large tan β value). These areas generally correspond with groundwater recharge areas (Hornberger and others, 1998). Inamdar (2009) defined high TWI values as ranging from 9 to 16 and low TWI values as ranging from 2 to 5.

The TWI relation is the basis of TOPMODEL and illustrates the model assumption of the subsurface water gradient being approximated by the slope of local surface topography. In TOPMODEL, the TWI is used to group hydrologically similar areas in the watershed and calculations are then performed in a semidistributed manner. To do so, the cells from the DEM are distributed in a histogram with each bin of cells (histogram interval) treated as a group based on the mean value of that bin (Williamson and others, 2009). The cells from each bin are treated the same for future calculations based on the principle that all cells having a similar TWI will have a similar hydrologic response (Beven and Kirby, 1979).

For this investigation, the TWI was computed using a 1/3 arc-second DEM from the National Elevation Dataset (NED) (Gesch and others, 2002). Processing was completed using Esri's Geographic Information System (GIS), ArcGIS. The NHD was used to burn streams into the DEM to ensure correct flow direction. Cells in the DEM that were lower than surrounding cells, called sinks, were filled and flow direction and accumulation were then determined. Slope, in degrees, was determined by applying the raw DEM, and instances of zero slope were replaced with 0.01 in order to calculate the TWI. The TWI was then calculated with the Arc Map raster calculator using the natural log of the upslope contributing area per unit contour length, divided by the slope ratio. Next, the raster to ASCII tool was used to export the raster data to a text file format for processing into the frequency distributions with the histogram builder as described by Williamson and others (2009). The relative frequency distributions of the TWI were computed using 30 equal-width bins. The stream network was excluded from the TWI analysis because the high values for surface water do not reflect the hillslope processes (Quinn and others, 1997).

Streamflow

Streamflow data used in this investigation were collected at station 02175000. As noted earlier, the USGS has been monitoring daily mean flow at this station since January 1939. Streamflow data used in the analysis for this investigation were collected continuously at 15-minute intervals from June 2007 to September 2009 using techniques described by Sauer and Turnipseed (2010). The process involved measuring water level (or stage) on a continuous basis and making a series of streamflow measurements throughout the range of observed stage. The collected data were then used to develop a stage–streamflow relation (also known as a rating curve) that was used to estimate streamflow from measured stage. Once the stage-streamflow relation was developed, periodic measurements were made on a regular basis to verify its accuracy, and as necessary, adjustments (or shifts) to the stage record were applied to account for deviations from the stage–streamflow relation.

TOPMODEL Streamflow Simulations

The application of TOPMODEL in the Edisto River Basin was done in a step-wise manner. The initial simulation was done using watershed characteristics for the Edisto River Basin, along with the calibrated parameters, meteorological data, and the TWI histogram from the TOPMODEL setup for McTier Creek near New Holland (hereafter referred to as the McTier Creek model) as described by Feaster and others (2010). The same goodness-of-fit statistics used by Feaster and others (2010, 2012) were used in this report to compare the various streamflow simulations with the observed streamflow data. Those statistics were (1) the Nash-Sutcliffe coefficient of model-fit efficiency (*NSE*) (Nash and Sutcliffe, 1970), (2) Pearson's correlation coefficient (*r*), (3) bias, (4) percent bias (*PBIAS*), (5) the root mean square error (*RMSE*), and (6) the mean absolute error (*MAE*).

The *NSE* is calculated as

$$NSE = \frac{\sum_{i=1}^{n}(Qo_i - Qo)^2 - \sum_{i=1}^{n}(Qo_i - Qs_i)^2}{\sum_{i=1}^{n}(Qo_i - Qo)^2}, \tag{4}$$

where

Qo_i is the observed flow for time step *i*,
Qo is the mean observed flow for the simulation period,
Qs_i is the simulated flow for time step *i*, and
n is the number of time steps in the simulation period.

An *NSE* value of 1.0 would indicate a perfect fit between the observed and simulated data, and a value of zero or less would indicate that using the mean of the observed data would be a better predictor than the model (Krause and others, 2005).

Pearson's *r* is calculated as

$$r = \frac{\sum_{i=1}^{n}(Qo_i - Qo)(Qs_i - Qs)}{\left[\sum_{i=1}^{n}(Qo_i - Qo)^2 \sum_{i=1}^{n}(Qs_i - Qs)^2\right]^{1/2}}, \tag{5}$$

where *Qs* is the mean simulated flow for the simulation period, and other variables are as previously defined. Pearson's *r* is one of the most commonly used measures of correlation and is called the linear correlation coefficient because it measures the linear association between two datasets (Helsel and Hirsch, 1995). If the data lie exactly along a straight line having a positive slope, then *r* is 1.

The bias is calculated as

$$\text{bias} = \frac{\sum_{i=1}^{n} Qs_i - Qo_i}{n}, \quad (6)$$

where the variables are as previously defined. The bias is the mean of the residuals between the simulated and observed data. The bias indicates whether the model is, on average, overpredicting or underpredicting the value being assessed.

Bias also can be presented in a percentage form (Moriasi and others, 2007) as

$$PBIAS = \left[\frac{\sum_{i=1}^{n} Qs_i - Qo_i}{\sum_{i=1}^{n} Qo_i} \right] \times 100, \quad (7)$$

where *PBIAS* is percent bias and measures the average tendency of the simulated data to be larger or smaller than the observed data and expressed as a percentage, and the other variables are as previously defined. The optimal value of *PBIAS* is zero, with low-magnitude values indicating an accurate model simulation. In this formulation of *PBIAS*, positive values indicate model overestimation and negative values indicate model underestimation.

Although the bias is a useful statistic, it can conceal large absolute differences between the observed and simulated data. That is, a bias of zero only indicates that the model is equally overpredicting and underpredicting but provides no information on the magnitude of such predictions. One approach to assessing such differences is by computing the variance, which is the average square of the residuals (Norman and Streiner, 1997). Because the variance is not expressed in the units of the original data, however, it is difficult to interpret. Alternatively, the square root of the variance (*RMSE*) is expressed in the units of the original data. The *RMSE* represents the mean of the absolute distance between the observed and simulated values. A low *RMSE* value indicates a close fit between the observed and simulated data. The *RMSE* is calculated as

$$RMSE = \sqrt{\frac{\sum (Qs_i - Qo_i)^2}{n}}, \quad (8)$$

where the variables are as previously defined.

Janssen and Heuberger (1993) noted that the *RMSE* also is sensitive to outliers because the differences between observed and simulated data are squared. The *MAE* is less sensitive to outliers and is similar to the bias except that it is the mean of the absolute value of the residuals as opposed to the mean of the actual residuals. Thus, the *MAE* provides the average of the magnitude of the residuals. In general, the *RMSE* can be expected to be greater than or equal to *MAE* for the range of most values. The degree to which the *RMSE* exceeds the *MAE* indicates the extent to which outliers exist in the data (Legates and McCabe, 1999). The *MAE* is calculated as

$$MAE = \frac{\sum_{i=1}^{n} | Qs_i - Qo_i |}{n}, \quad (9)$$

where the variables are as previously defined.

In addition to the goodness-of-fit statistics, single-mass curves for the assessment periods also were used for graphical comparisons of various simulations. The single-mass curve depicts the cumulative daily mean flow and, therefore, represents the cumulative volume of daily mean flow for the period being analyzed. The slope of the curve indicates the hydrologic conditions represented. A steep slope indicates wet conditions, a flat slope indicates dry conditions, and a substantial change in slope indicates a change in the hydrologic regime. Additionally, flow-duration curves of simulated and observed daily mean flows were plotted and reviewed; these curves represent the percentage of time that a specified flow is equaled or exceeded during a given time period (Searcy, 1959).

Streamflow Routing

For the McTier Creek TOPMODEL flow simulations, the routing functions of the model were not used because the traveltime through the watershed was less than the simulation time step. For the Edisto River Basin, however, the traveltime (days to weeks) is such that routing is warranted.

For the routing function in TOPMODEL and after streamflow is generated, a simple algorithm is used to account for traveltime from the point of generation to the basin outlet (Kennen and others, 2008). The instream distance from each cell of the DEM to the basin outlet is computed by using the flow length tool in ArcGIS. This distance is multiplied by an estimate of the velocity of the flow in the channel to obtain the traveltime. The traveltime is divided by the length of a single time step and is rounded down to an integer, which equals the number of time steps the flow will be delayed in reaching the basin outlet. The zonal statistics feature in ArcGIS is used to compute the percentage of the basin associated with each time-step delay. Flow at the basin outlet for any given time step is computed as the sum of (1) the total flow generated in the given time step multiplied by the percentage of the basin having no delay and (2) the delayed flows from previous time steps.

Streamflow Simulation Results

The streamflow simulations for the Edisto River were done in a step-wise manner, starting with applying calibrated TOPMODEL parameters, TWI data, and meteorological data from the McTier Creek model (Feaster and others, 2010, 2012) to the Edisto River model. Additional data from the Edisto River were then applied, and lastly, the parameter estimation program (PEST) was used to help calibrate model parameters for the Edisto River model (Doherty, 2005). PEST, which also was used to calibrate the McTier Creek TOPMODEL, is a nonlinear parameter estimator that adjusts model parameters until the fit between simulated streamflow estimates and observed streamflow are optimized using a weighted least-squares scheme. If initial simulations using PEST indicated no change in a parameter from the value used in the McTier Creek TOPMODEL, the value was held constant in subsequent PEST runs. Table 3 provides information for each TOPMODEL simulation defining the input data sources used, table 4 lists the parameter values associated with those simulations, and table 5 lists the goodness-of-fit statistics for each simulation. Graphical comparisons of the various TOPMODEL simulated daily mean flows with the observed daily mean flows at station 02175000 for the period from June 13, 2007, to September 30, 2009, are shown in (fig. 8). In addition to the comparison of daily mean flows, graphical comparisons of single-mass and flow-duration curves also were made (figs. 9 and 10). As noted earlier, the TOPMODEL code being utilized uses the first year of simulations as a warm-up period. Consequently, the model was actually run from June 13, 2006, to September 30, 2007, but the model only provides simulation output from June 13, 2007, to September 30, 2009.

Simulation 1 was made using watershed characteristics computed from the Edisto River Basin along with calibrated parameters, TWI data, and meteorological data from the McTier Creek TOPMODEL calibration documented by Feaster and others (2012) (tables 3 and 4). The goodness-of-fit statistics along with the graphical comparisons show that the simulated data provided a poor fit to the observed data (table 5, figs. 8*A*, 9*A*, and 10*A*). The oversimulation of the peak flows along with the low *NSE* and *r* values was interpreted as an indication that the flood routing functions in TOPMODEL needed to be applied, which was to be expected given the size of the Edisto River Basin.

Simulation 2 used the same calibration parameters as simulation 1, except that the routing function in TOPMODEL was activated with an assumed velocity for routing water (subv) of 50 kilometers per day (table 4). Making that one change increased the *r* value from 0.60 to 0.83 and increased the *NSE* from –1.34 to –0.10, which can be attributed to the improvement in the timing and attenuation of the peak hydrographs because of flow routing. Comparison of the total volume from the simulations with the total volume from the observed data showed a percentage error of 65.8 and 63.9 percent for simulations 1 and 2, respectively. These results indicate that the simulations for the Edisto River generated by applying the calibrated parameters along with the TWI and meteorological data from the McTier Creek model resulted in relatively poor fit when compared to the observed daily mean flow data at station 02175000. It would be expected that the calibration parameters might be different and would need to be modified for a couple of reasons. First, the drainage area upstream of McTier Creek near New Holland is 30.7 mi^2, compared to the drainage upstream up for Edisto River near Givhans, which is 2,730 mi^2. Second,

Table 3. TOPMODEL simulation number and simulation description.

[TWI, topographic wetness index; McTier, McTier Creek basin with outlet at station 02172305, McTier Creek near New Holland, SC; IDW, inverse-distance weighting; GHCN, Global Historical Climatology Network; Edisto, Edisto River basin with outlet at station 02175000, Edisto River near Givhans, SC; NEXRAD, Next generation weather radar; PEST, Parameter ESTimation program]

Simulation	TWI source	Temperature source	Precipitation source	Calibration parameters	Streamflow routing
1	McTier	IDW GHCN McTier	IDW GHCN McTier	McTier	No
2	McTier	IDW GHCN McTier	IDW GHCN McTier	McTier	Yes
3	Edisto	IDW GHCN McTier	IDW GHCN McTier	McTier	Yes
4	Edisto	IDW GHCN McTier	NEXRAD Edisto	McTier	Yes
5	Edisto	IDW GHCN Edisto	IDW GHCN Edisto	McTier	Yes
6	Edisto	Thiessen GHCN Edisto	Thiessen GHCN Edisto	McTier	Yes
7	Edisto	Thiessen GHCN Edisto	NEXRAD Edisto	PEST	Yes
8	Edisto	IDW GHCN Edisto	IDW GHCN Edisto	PEST	Yes
9	Edisto	Thiessen GHCN Edisto	Thiessen GHCN Edisto	PEST	Yes

Table 4. Parameter values used for the TOPMODEL simulations for station 02175000, Edisto River near Givhans, SC.

[--, value was unchanged from previous simulation; NA, not applicable; TR55, Technical Release 55]

Model parameter	Parameter value for referenced simulation (table 3)								
	1	2	3	4	5	6	7	8	9
Total area (square kilometers)	7,058	--	--	--	--	--	--	--	--
Lake area (square kilometers)	18.6	--	--	--	--	--	--	--	--
Stream area (square kilometers)	86.1	--	--	--	--	--	--	--	--
Saturated conductivity (inches per hour)	3.87	--	--	--	--	--	--	--	--
Soil depth (inches)	66.3	--	--	--	--	--	--	--	--
Field capacity (unitless)	0.16	--	--	--	--	--	--	--	--
Water holding capacity (unitless)	0.10	--	--	--	--	--	--	--	--
Porosity (unitless)	0.367	--	--	--	--	--	--	--	--
Percent impervious	1.0	--	--	--	--	--	--	--	--
Percent road impervious	0.29	--	--	--	--	--	--	--	--
Latitude	33.028	--	--	--	--	--	--	--	--
Effective impervious (decimal percent)	0.8*	--	--	--	--	--	--	--	--
Conductivity multiplier	2.9*	--	--	--	--	--	--	--	--
Percent macropore (decimal percent)	0.5*	--	--	--	--	--	--	0.33†	0.5*
Scaling parameter (m)	45.0*	--	--	--	--	--	53.3†	52.4†	53.6†
subv	NA	50.0	--	--	--	--	29.1†	29.0†	--
Depth of root zone (meters)	1.9*	--	--	--	--	--	--	--	--
Impervious runoff constant	0.10*	--	--	--	--	--	--	--	--
TR55 curve number	98*	--	--	--	--	--	--	--	--
Uplake area (as a fraction of the total area)	0.27	--	--	--	--	--	--	--	--
Lake delay (unitless)	1.2*	--	--	--	--	--	--	--	--

*Values same as those from McTier Creek near New Holland TOPMODEL calibration (Feaster and others, 2012).

†Calibration using parameter estimation program (PEST).

Table 5. Goodness-of-fit statistics for TOPMODEL simulations at Edisto River near Givhans, SC, for June 13, 2007, to September 30, 2009.

[ft^3/s, cubic foot per second; --, not applicable; *PBIAS*, percent bias; *RMSE*, root mean square error; *MAE*, mean absolute error; *r*, Pearson's correlation coefficient; NSE, Nash-Sutcliffe coefficient of model-fit efficiency]

Statistic	Observed	Simulation number (table 3)								
		1	2	3	4	5	6	7	8	9
Maximum (ft^3/s)	4,740	13,800	6,410	9,740	5,810	7,300	7,700	4,140	5,600	6,090
Mean (ft^3/s)	1,160	1,920	1,900	1,270	946	1,380	1,350	1,150	1,500	1,670
Median (ft^3/s)	762	1,420	1,500	453	455	861	652	848	1,190	1,290
Minimum (ft^3/s)	219	648	718	66	75	95	100	203	194	281
Standard deviation (ft^3/s)	926	1,490	1,120	1,700	1,120	1,440	1,570	854	1,200	1,320
Bias (ft^3/s)	--	763	741	113	–213	217	191	–8.5	344	509
PBIAS (percent)	--	39.7	39.0	8.9	–22.6	15.8	14.2	–0.7	22.9	30.5
RMSE (ft^3/s)	--	1,410	970	1,120	699	889	956	431	784	858
MAE (ft^3/s)	--	854	797	684	498	559	617	310	501	572
r	--	0.60	0.83	0.79	0.81	0.82	0.84	0.89	0.81	0.87
NSE	--	–1.34	–0.10	–0.48	0.43	0.08	–0.07	0.78	0.28	0.14
Percentage error in total volume	--	65.8	63.9	–18.4	–18.4	18.7	16.5	–0.7	29.6	43.9

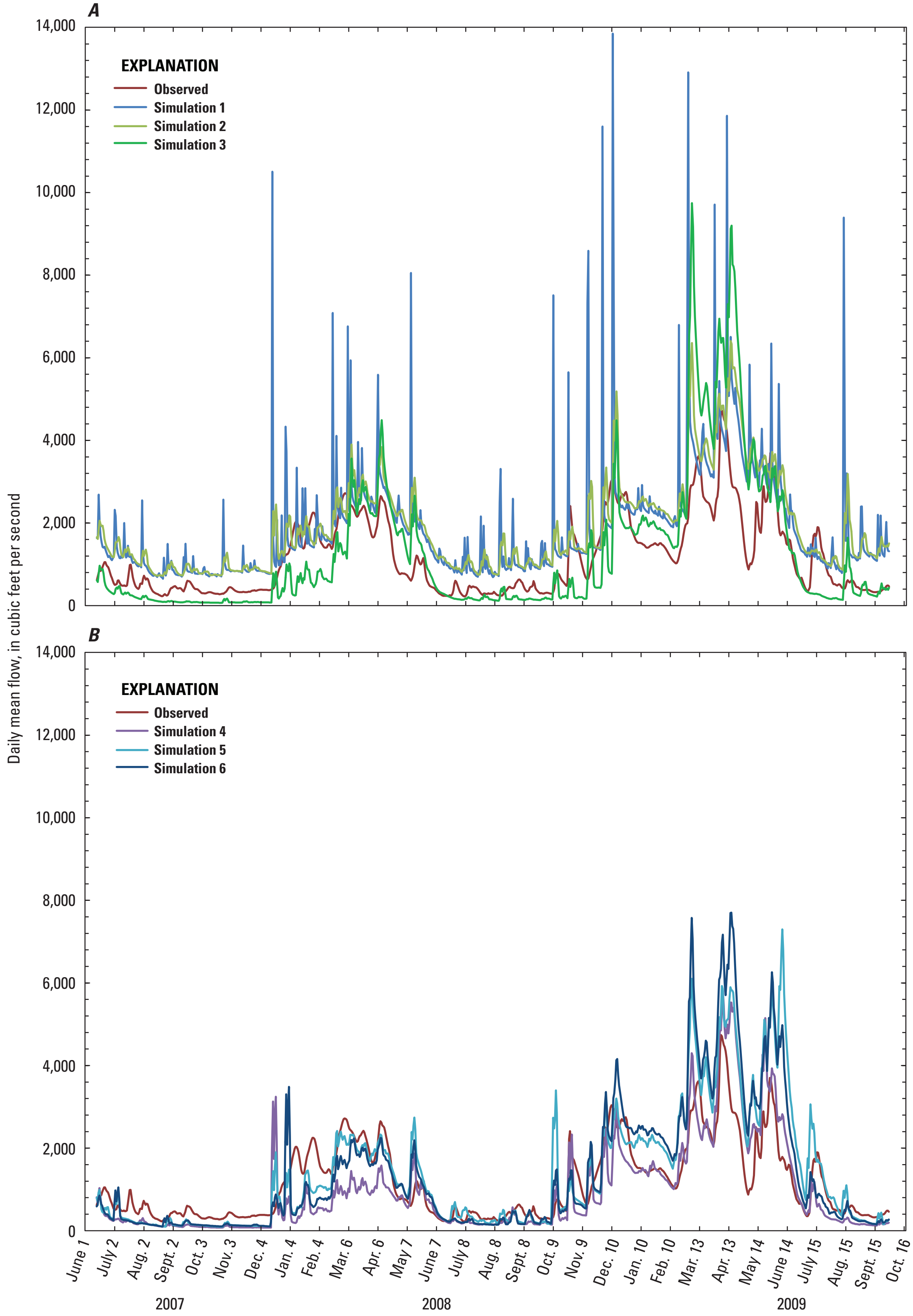

Figure 8. Simulated and observed daily mean flow at station 02175000, Edisto River near Givhans, SC, for the period from June 13, 2007, to September 30, 2009, for (*A*) simulation numbers 1, 2, and 3; (*B*) simulation numbers 4, 5, and 6; (*C*) simulation numbers 7, 8, and 9; and (*D*) simulation number 7.

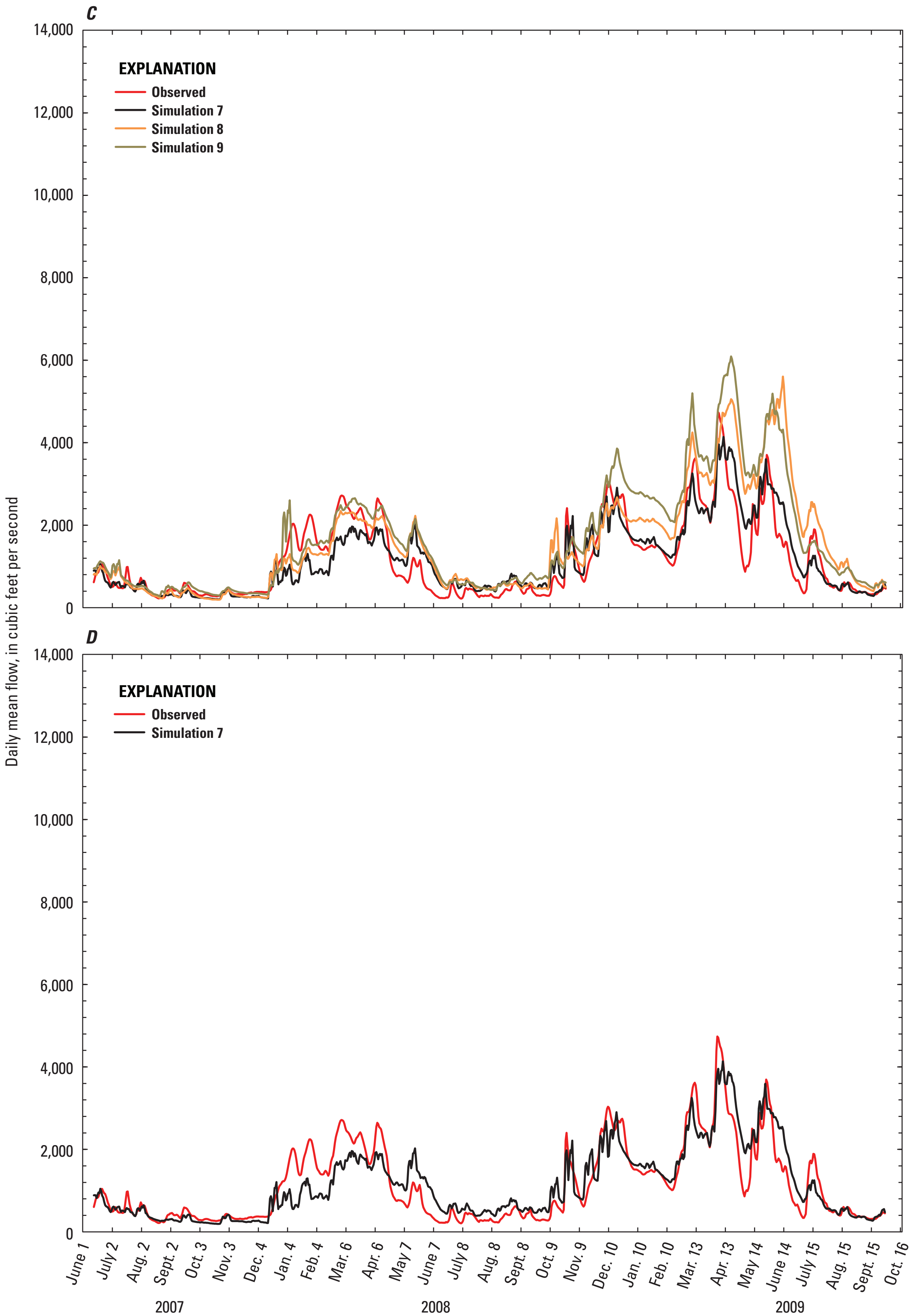

Figure 8. Simulated and observed daily mean flow at station 02175000, Edisto River near Givhans, SC, for the period from June 13, 2007, to September 30, 2009, for (*A*) simulation numbers 1, 2, and 3; (*B*) simulation numbers 4, 5, and 6; (*C*) simulation numbers 7, 8, and 9; and (*D*) simulation number 7.—Continued

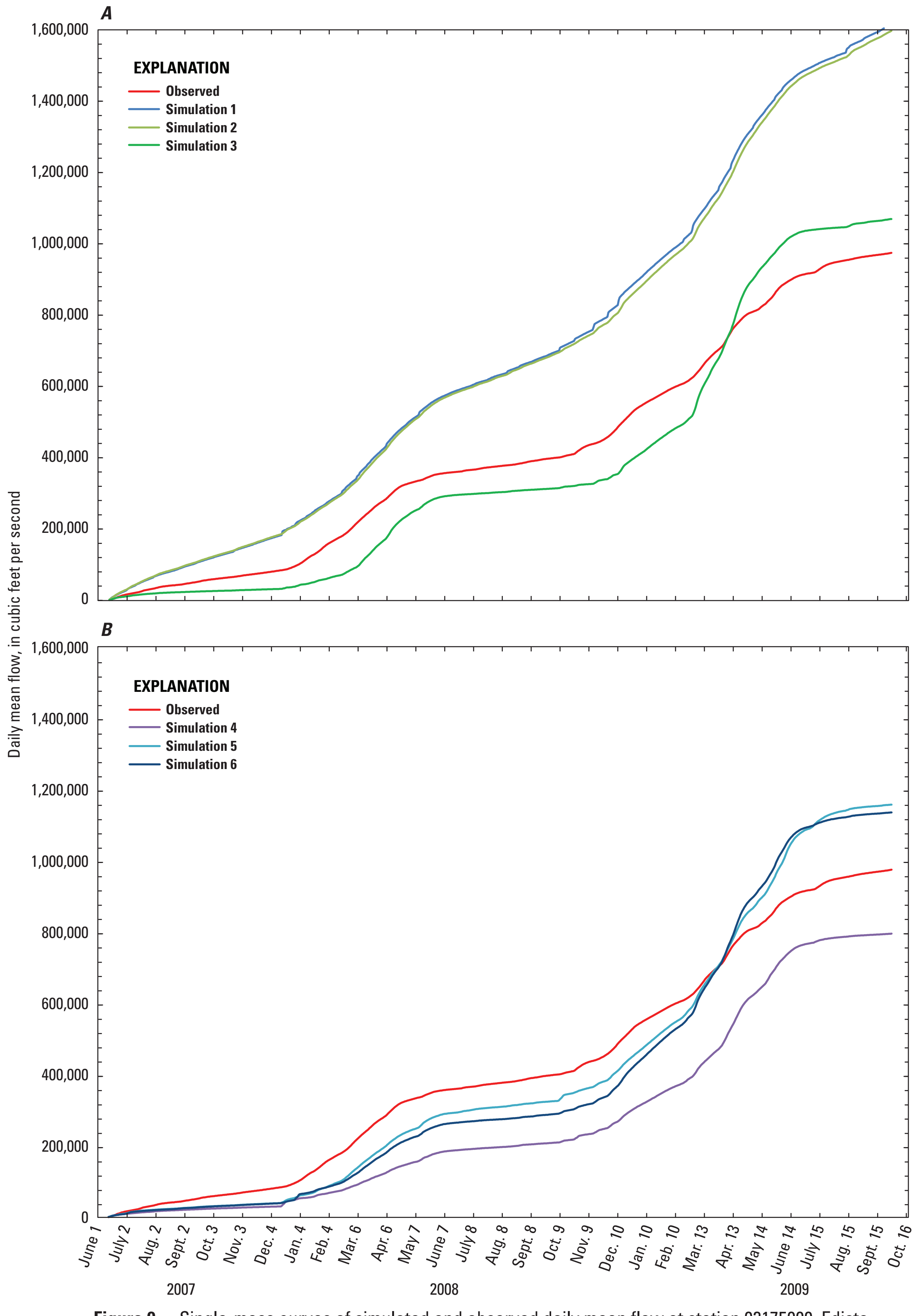

Figure 9. Single-mass curves of simulated and observed daily mean flow at station 02175000, Edisto River near Givhans, SC, for the period of June 13, 2007, to September 30, 2009, for (*A*) simulation numbers 1, 2, 3; (*B*) simulation numbers 4, 5, and 6; and (*C*) simulation numbers 7, 8, and 9.

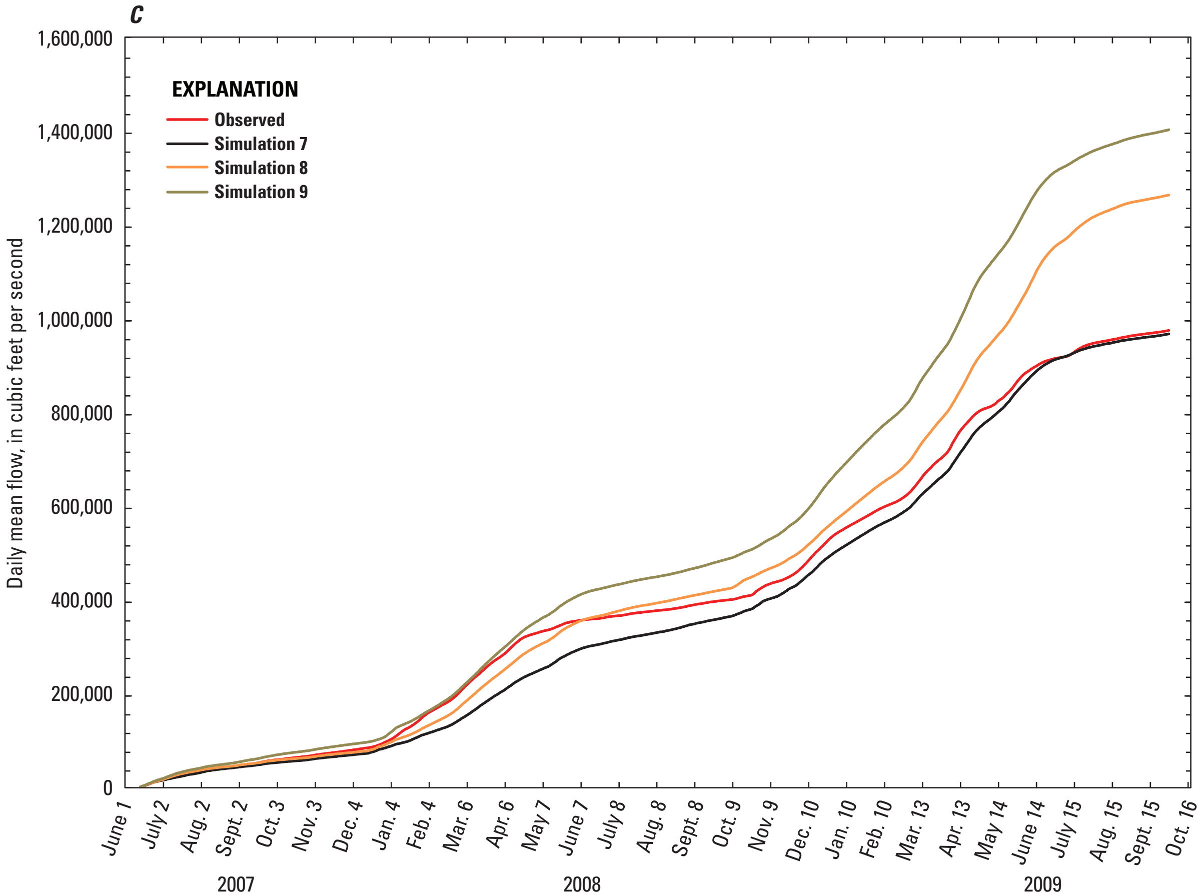

Figure 9. Single-mass curves of simulated and observed daily mean flow at station 02175000, Edisto River near Givhans, SC, for the period of June 13, 2007, to September 30, 2009, for (*A*) simulation numbers 1, 2, 3; (*B*) simulation numbers 4, 5, and 6; and (*C*) simulation numbers 7, 8, and 9.—Continued

the McTier Creek Basin is located completely within the Sand Hills ecoregion of South Carolina, whereas the Edisto River near Givhans basin drains about 31 percent from the Sand Hills ecoregion and 69 percent from the Coastal Plain (Feaster and others, 2009). In addition, for large basins, applying uniform rainfall data across the basin also could account for some uncertainty in the simulations. Moreover, given the significant difference in the size of the basins, some differences in the TWI data would be expected as well.

Simulation 3 used the same model parameters and meteorological data as simulation 2 but used the TWI data computed for the Edisto River Basin instead of the TWI data from the McTier Creek Basin (table 3). As shown in the graphical comparisons and the goodness-of-fit statistics, this change resulted in a substantial reduction in the overall flow volume (fig. 8*A*, 9*A*, and 10*A*; table 5).

Simulation 4 used the same model parameters as simulation 3, as well as the TWI data from the Edisto River Basin, but used NEXRAD precipitation data generated for the Edisto River Basin instead of the precipitation data that had been used in the McTier Creek Basin TOPMODEL (fig. 7*A*, tables 1 and 3; Feaster and others, 2012). Using the NEXRAD precipitation did not substantially affect the correlation coefficient or the error in total volume but greatly improved the *RMSE* and *NSE* (fig. 8*B*–*C*, table 5).

Simulation 5 was made using the IDW GHCN meteorological data from in and around the Edisto River Basin along with the TWI data from the Edisto River Basin but with TOPMODEL calibrated parameters from the McTier Creek model (table 3). The goodness-of-fit statistics indicated an increase in total volume (as indicated by the percentage of error in total volume increasing from –18.4 to 18.7) and a substantial reduction in *NSE* from 0.43 to 0.08 (table 5, figs. 8*B*, 9*B*, and 10*B*).

Simulation 6 used the same calibration parameters as simulation 5, except GHCN meteorological data from stations in and around the Edisto River Basin weighted using Thiessen polygons in place of the IDW GHCN meteorological data (table 3). The goodness-of-fit statistics were slightly worse for *RMSE*, *MAE*, and *NSE* and slightly improved for bias, *PBIAS*, *r*, and percentage error in total volume (table 5, figs. 8*B*, 9*B*, and 10*B*).

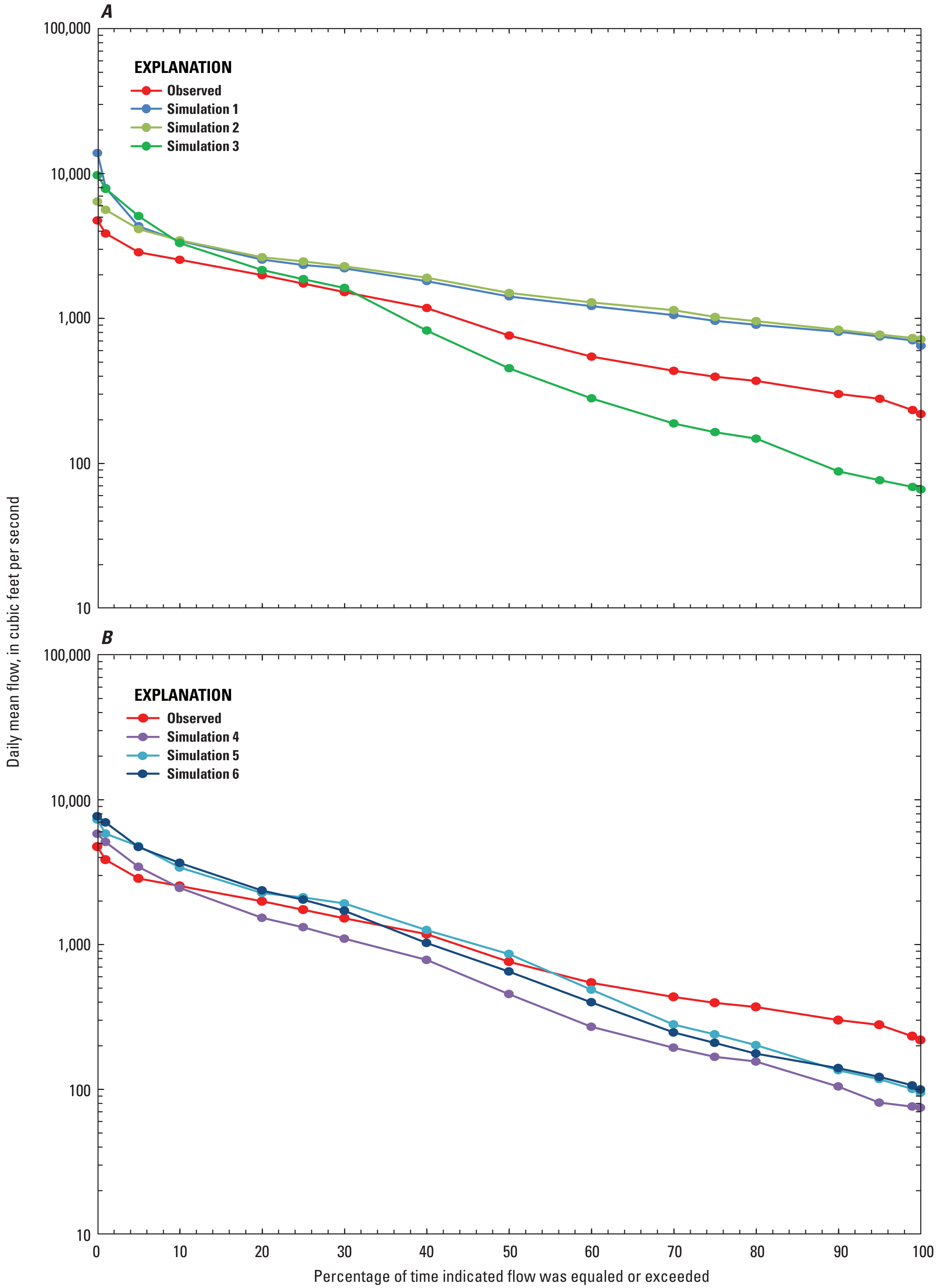

Figure 10. Flow-duration curves of simulated and observed daily mean flow at station 02175000, Edisto River near Givhans, SC, for the period from June 13, 2007, to September 30, 2009, for (*A*) simulation numbers 1, 2, and 3; (*B*) simulation numbers 4, 5, and 6; and (*C*) simulation numbers 7, 8, and 9.

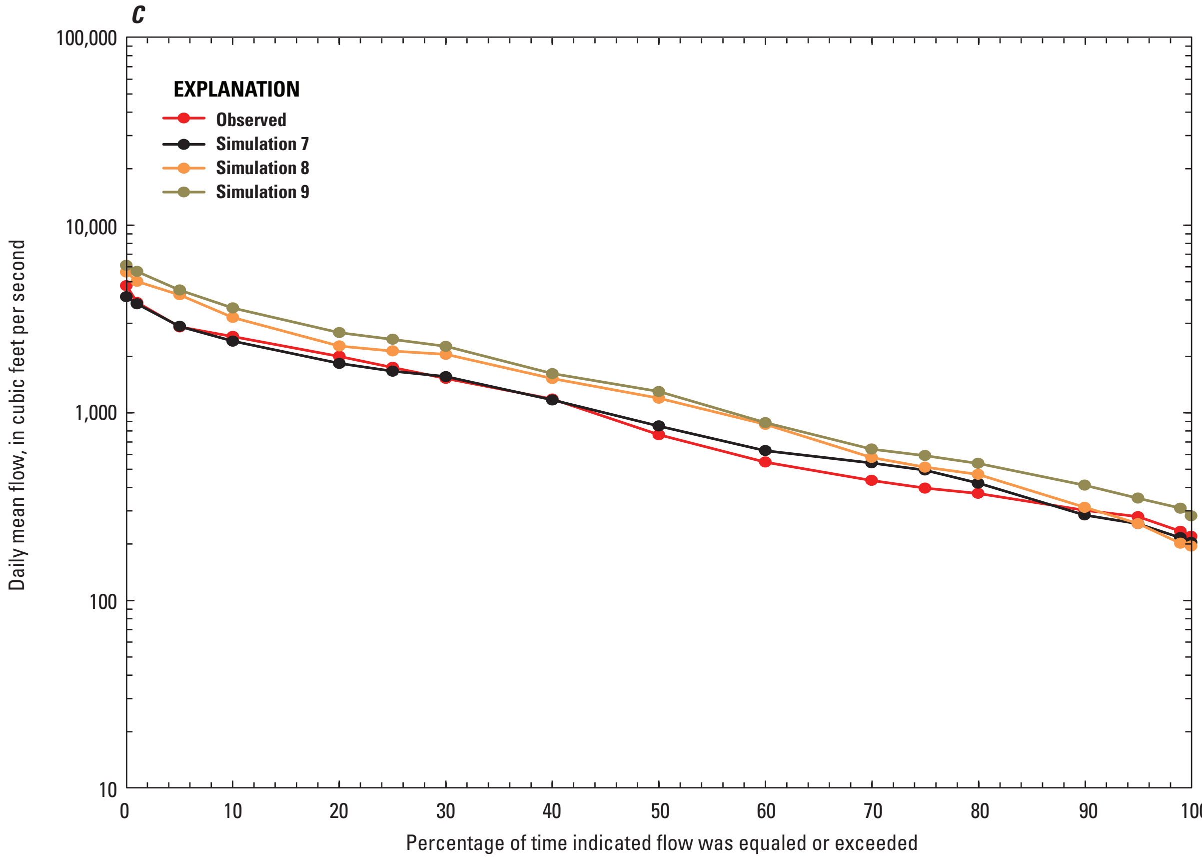

Figure 10. Flow-duration curves of simulated and observed daily mean flow at station 02175000, Edisto River near Givhans, SC, for the period from June 13, 2007, to September 30, 2009, for (*A*) simulation numbers 1, 2, and 3; (*B*) simulation numbers 4, 5, and 6; and (*C*) simulation numbers 7, 8, and 9.—Continued

As indicated by the goodness-of-fit statistics and graphical comparisons for simulations 1 through 6, simply applying the calibrated TOPMODEL parameters from the McTier Creek model to the Edisto River model produced mediocre results at best with respect to matching the observed daily mean flows at station 02175000. Thus, the next step was to use PEST (Doherty, 2005) to determine if the simulation results could be improved. For each set of meteorological data for the Edisto River Basin (NEXRAD, IDW GHCN, and Thiessen polygon GHCN), initial simulations were made allowing PEST to adjust all calibration parameters that had previously been calibrated in the McTier Creek TOPMODEL (simulation 7, 8, and 9, respectively; table 4). Although routing (subv) was not included in the McTier Creek model, most of the other calibration parameters common to both models had the same calibrated values (table 4). From those initial simulations, PEST indicated that adjusting values for the scaling parameter (*m*) and subv provided the most improved simulation results (table 5). For simulation 8, which used IDW GHCN meteorological data, percent macropore also was modified from the value used in the McTier Creek model (table 4).

The goodness-of-fit statistics from simulation 7 indicate that using the NEXRAD precipitation data for the Edisto River Basin provided the best overall simulation, with an *NSE* of 0.78, *r* of 0.89, *PBIAS* of –0.7 percent, and a total simulated volume differing by only –0.7 percent (table 5, figs. 8*C*–*D*, 9*C*, and 10*C*). These results were even better than the TOPMODEL results for McTier Creek near New Holland, a much smaller drainage basin, which had a *NSE* of 0.67, *r* of 0.82, and *PBIAS* of 0.31 percent for the simulation using measured rainfall data and an *NSE* of 0.68, *r* of 0.85, and *PBIAS* of –0.87 percent using NEXRAD rainfall data (Feaster and others, 2012). Concerning the NEXRAD rainfall data providing the best simulation results, this outcome may be related to the size of the Edisto River Basin. Specifically, the NEXRAD rainfall data are generated from a much finer and consistent grid than those used for the IDW and Thiessen polygon weighting methods (fig. 3). For such a large basin, the NEXRAD rainfall is therefore likely to better reflect the overall “average” rainfall.

Edisto River Data Viewer for Flows and Water-Quality Loads

Benedict and others (2012) developed the McTier Creek Data Viewer to assist in visualizing the abundant hydrologic and water-quality data associated with the McTier Creek watershed mercury investigation. Using the same digital platform developed for the McTier Creek Data Viewer, the Edisto River Data Viewer was developed as part of this investigation. The Edisto River Data Viewer consists of a set of Microsoft Excel spreadsheets that incorporate selected measured and modeled data at station 02175000 for the same period used in the McTier Creek investigation (June 2007 to August 2009). Applications within the Edisto River Data Viewer provide a means for visualizing selected data trends using graphs that display (1) time-series plots and scatterplots of selected hydrologic and water-quality data, (2) seasonal trends associated with selected water-quality constituents, and (3) comparison plots of selected model simulations. The scope of the Edisto River investigation, which only included 9 water-quality sampling events, was not as extensive as that for McTier Creek, which included 45 events. Additionally, some of the hydrologic and water-quality models developed for McTier Creek, such as the grid-based mercury model (GBMM) and Visualizing Ecosystems for Land Management Assessment model (VELMA), have not been developed for the Edisto River. Therefore, some of the data placeholders in the Edisto River Data Viewer were left blank because the data were not available. A list of the measured and modeled data included in the Edisto River Data Viewer is provided in tables 6 through 8. Worksheets and applications that compose the Edisto River Data Viewer are listed in table 9. A screen capture of the "Title Sheet" worksheet in the Edisto River Data Viewer Microsoft Excel application is shown on figure 11. Additional information regarding the platform originally developed for the McTier Creek Data Viewer and adapted for use in the Edisto River Data Viewer can be found in Benedict and others (2012). The water-quality load models incorporated into the Edisto River Data Viewer include TOPLOAD, TOPLOAD–H, and the Load Estimator (LOADEST) models. A brief description of these models follows.

TOPLOAD and TOPLOAD–H

The version of TOPMODEL applied to the McTier Creek (Feaster and others, 2010) and Edisto River Basins does not include a mass-balance algorithm for evaluating water-quality loads. Such an algorithm can be applied explicitly to the TOPMODEL hydrologic simulations, however, resulting in a simple water-quality load model. Using the TOPMODEL output and the simple mass-balance relation shown in equation 10, Benedict and others (2012) developed a spreadsheet application within the McTier Creek Data Viewer for computing water-quality loads associated with a given water-quality constituent. As discussed earlier, calibration of TOPMODEL was based on streamflow at the outlet of the basin and thus, individual flow components were not verified. For the best simulation run (simulation 7), the TOPMODEL output indicated that about 86 percent of the total streamflow was attributed to Q_{qret}, the subsurface return flow.

$$LOAD = Q_{qb}C_{qb} + Q_{qret}C_{qret} + Q_{qinf}C_{qinf} + Q_{qimp}C_{qimp} + Q_{qsrip}C_{qsrip} + Q_{qof}C_{qof}, \tag{10}$$

where:

LOAD is the simulated daily average watershed load associated with a given water-quality constituent, in mass per day;

Q_{qb} is subsurface base flow from TOPMODEL, in cubic feet per second;

C_{qb} is water-quality constituent concentration for subsurface base flow, in mass per liter;

Q_{qret} is subsurface return flow from TOPMODEL, in cubic feet per second;

C_{qret} is water-quality constituent concentration for subsurface return flow, in mass per liter;

Q_{qinf} is surface infiltration-excess overland flow from TOPMODEL, in cubic feet per second;

C_{qinf} is water-quality constituent concentration for surface infiltration-excess overland flow, in mass per liter;

Q_{qimp} is surface impervious flow from TOPMODEL, in cubic feet per second;

C_{qimp} is water-quality constituent concentration for surface impervious flow, in mass per liter;

Q_{qsrip} is surface open-water body flow from TOPMODEL, in cubic feet per second;

C_{qsrip} is water-quality constituent concentration for surface open-water body flow, in mass per liter;

Q_{qof} is surface overland saturation flow from TOPMODEL, in cubic feet per second; and

C_{qof} is water-quality constituent concentration for surface overland saturation flow, in mass per liter.

Several variants of this load model were developed, with the first being TOPLOAD, which utilized the simulated surface and subsurface flow components taken directly from TOPMODEL as implied in equation 10. The second variant, TOPLOAD–H, includes a groundwater partitioning algorithm presented in Hornberger and others (1994) that was added to the summed subsurface flow components of TOPMODEL (summation of Q_{qret} and Q_{qb}), thereby providing for multiple groundwater flow components. The algorithm for TOPLOAD–H requires estimates of the total soil depth and the soil porosity, which are taken directly from the TOPMODEL input data, and the depth of the upper soil horizon, which is assigned by the user's judgment. The water-quality constituent concentrations for

Table 6. Measured instream hydrologic and water-quality data included in the Edisto River Data Viewer collected at streamgaging station 02175000, Edisto River near Givhans, SC, June 2007 to August 2009.

[DOC, dissolved organic carbon]

Constituent	Units
Time-series hydrologic data	
Streamflow	Cubic feet per second
Discrete instream water-quality data	
Air temperature	Degrees Celsius
Water temperature	Degrees Celsius
Field pH	Standard units
Field specific conductance	Microsiemens per centimeter
Laboratory specific conductance	Microsiemens per centimeter
Laboratory alkalinity	Milligrams per liter as calcium carbonate
Dissolved ammonia	Milligrams per liter
Dissolved calcium	Milligrams per liter
Dissolved chloride	Milligrams per liter
Dissolved iron	Micrograms per liter
Dissolved magnesium	Milligrams per liter
Dissolved nitrate plus nitrite	Milligrams per liter
Dissolved nitrite	Milligrams per liter
Dissolved organic carbon	Milligrams per liter
Dissolved orthophosphate	Milligrams per liter
Dissolved oxygen concentration	Milligrams per liter
Dissolved potassium	Milligrams per liter
Dissolved sodium	Milligrams per liter
Dissolved sulfate	Milligrams per liter
Total nitrogen	Milligrams per liter
Total phosphorus	Milligrams per liter
Suspended inorganic carbon	Milligrams per liter
Suspended organic carbon	Milligrams per liter
Suspended sediment	Milligrams per liter
Suspended sediment finer than 63 microns	Percent
Suspended total carbon	Milligrams per liter
Suspended total nitrogen	Milligrams per liter

Table 6. Measured instream hydrologic and water-quality data included in the Edisto River Data Viewer collected at streamgaging station 02175000, Edisto River near Givhans, SC, June 2007 to August 2009.—Continued

[DOC, dissolved organic carbon]

Constituent	Units
Discrete in-stream water-quality data—Continued	
Filtered methylmercury	Nanograms per liter
Filtered total mercury	Nanograms per liter
Particulate methylmercury	Nanograms per liter
Particulate total mercury	Nanograms per liter
Total mercury (filtered plus particulate total mercury)	Nanograms per liter
Hydrophilic acid to specific ultraviolet absorbance ratio	Fraction
Hydrophilic acids	Percent
Hydrophobic organic acid to specific ultraviolet absorbance ratio	Fraction
Hydrophobic organic acids	Percent
Transphillic acid to specific ultraviolet absorbance ratio	Fraction
Transphillic acids	Percent
Time-series hydrologic data	
Streamflow	Cubic feet per second
Discrete in-stream water-quality data	
Ash-free phytoplankton biomass	Milligrams per liter
Chlorophyll *a*	Micrograms per liter
Pheophytin *a*	Micrograms per liter
Phytoplankton biomass as ash weight	Milligrams per liter
Phytoplankton biomass as dry weight	Milligrams per liter
Computed ultraviolet absorbance at 254 nanometers	Per centimeter (corrected for iron concentration)
Specific ultraviolet absorbance	Milligrams per liter DOC per meter
Ultraviolet absorbance at 254 nanometers	Per centimeter
Ultraviolet absorbance at 365 nanometers	Per centimeter

both TOPLOAD and TOPLOAD–H also must be assigned by the user on the basis of field observations and (or) judgment. Although TOPLOAD and TOPLOAD–H were primarily developed to assess mercury loads, they also can be applied to other water-quality constituents. Only the loads associated with total mercury were included in the Edisto River Data Viewer. A more in-depth discussion of the derivation of TOPLOAD and TOPLOAD–H is provided in the appendix of Benedict and others (2012).

To apply TOPLOAD and TOPLOAD–H to assess total mercury loads at station 02175000, the TOPMODEL flow components (as defined in equation 10) from simulation 7 (tables 3, 4, and 5) were imported into the Edisto River Data Viewer and applied to the TOPLOAD and TOPLOAD–H spreadsheets. Concentrations (as defined in equation 10) for total mercury were then assigned to each flow component. Typically, these concentrations are defined from limited field measurements. Because a primary focus of this investigation was on scaling up TOPMODEL, TOPLOAD, and TOPLOAD–H from the small headwater basin of McTier Creek to the larger Edisto River Basin, the concentrations used in the McTier Creek TOPLOAD and TOPLOAD–H models (Benedict and others, 2012; Golden and others, 2012) also were used in the Edisto River TOPLOAD and TOPLOAD–H models. A total mercury concentration of 5 nanograms per liter (ng/L) was assigned to each of the flow components in the Edisto River TOPLOAD and TOPLOAD–H models. This value represents the average daily concentration for all flows (low, high, and base flow), based on field measurements from the 45 sampling days during the simulation period and informed judgment. Results for the TOPLOAD and TOPLOAD–H models were incorporated into the Edisto River Data Viewer.

Load Estimator (LOADEST)

Journey and others (2012) computed loads for mercury, DOC, dissolved chloride, dissolved sulfate, and suspended-sediment in the Edisto River Basin using the S–LOADEST (Lorenz and others, 2011) plug-in for TIBCO Spotfire S+ 8.1 software

Table 7. Simulated hydrologic time-series data included in the Edisto River Data Viewer for streamgaging station 02175000, Edisto River near Givhans, SC.

[Selected TOPMODEL output (Wolock, 1993; Feaster and others, 2010). Simulation period: June 13, 2007, through September 30, 2009. TOPMODEL, Topography-Based Hydrological Model]

Variable	Variable definition	Units
acsat	Percent of the area predicted to be saturated	Percent
aversz	Average (over all wetness index bins) storage in the root zone	Millimeters per day
avesuz	Average (over all wetness index bins) storage in the unsaturated zone	Millimeters per day
pet	Potential evapotranspiration	Millimeters per day
pettot	Actual evapotranspiration	Millimeters per day
ppt	Precipitation	Millimeters per day
qb	Base flow	Millimeters per day
qimp	Flow from impervious areas	Millimeters per day
qinf	Infiltration excess	Millimeters per day
qof	Overland flow	Millimeters per day
qpred	Total predicted flow at basin outlet	Millimeters per day
qret	Return flow	Millimeters per day
qrip	Flow from open-water bodies	Millimeters per day
quz	Flow in unsaturated zone	Millimeters per day
s	Average saturation deficit	Millimeters per day

Table 8. Simulated time-series water-quality load data included in the Edisto River Data Viewer for streamgaging station 02175000, Edisto River near Givhans, SC.

[TOPLOAD, Water-quality load model developed from TOPMODEL; TOPLOAD-H, Water-quality load model developed from TOPMODEL with Hornberger's (Hornberger and others, 1994) groundwater partitioning algorithm]

Constituent	Units
TOPLOAD and TOPLOAD-H (Benedict and others, 2012) Simulation period: June 13, 2007, through September 30, 2009	
Dissolved calcium	Kilograms per day
Dissolved chloride	Kilograms per day
Dissolved sulfate	Kilograms per day
Filtered total mercury	Milligrams per day
Dissolved sodium	Kilograms per day
Dissolved organic carbon	Kilograms per day
Total mercury (filtered plus particulate)	Milligrams per day
LOADEST (Runkel and others, 2004) Simulation period: October 2004 through September 2009	
Filtered methylmercury	Milligrams per day
Filtered total mercury	Milligrams per day
Particulate total mercury	Milligrams per day
Particulate methylmercury	Milligrams per day
Total mercury (filtered plus particulate)	Milligrams per day
Dissolved organic carbon	Milligrams per day
Suspended sediment	Kilograms per day
Particulate organic carbon	Kilograms per day
Dissolved chloride	Kilograms per day
Dissolved sulfate	Kilograms per day

(TIBCO Spotfire Co., Palo Alto, Calif.). S–LOADEST is derived from LOADEST, a FORTRAN program that has been used extensively for estimating constituent loads in streams and rivers (Runkel and others, 2004). S–LOADEST allows the user to estimate annual, monthly, and seasonal constituent loads using a regression (rating curve) approach (Cohn, 2005). The regression model computes daily loads based on relations between constituent load and explanatory variables that are functions of streamflow and time. The time component can be represented as increasing and decreasing trends over time and as seasonal changes.

Instantaneous constituent loads are computed using the following equation:

$$L_{Hg} = C_{Hg} * Q_i * C_l, \tag{11}$$

where

L_{Hg} is the mercury species (or other constituent of interest) load at the time of sampling, in milligrams per day;

C_{Hg} is the concentration of the mercury species (or other constituent of interest), in nanograms per liter;

Q_i is the instantaneous streamflow at the time of sampling, in cubic feet per second; and

C_l is a unit conversion factor (2.447).

Table 9. Description of selected worksheets and applications included in the Edisto River Data Viewer.

[TOPMODEL, topography-based hydrological model; TOPLOAD, Water-quality load model developed from TOPMODEL; TOPLOAD-H, Water-quality load model developed from TOPMODEL with Hornberger’s (Hornberger and others, 1994) groundwater partitioning algorithm; GBMM, Grid-Based Mercury Model; VELMA, Visualizing Ecosystems for Land Management Assessment Model]

Worksheet name	Description
Title Sheet	Title sheet for data viewer.
Release Notes	References and selected information associated with hydrologic and water-quality models used in the data viewer and a description of each worksheet in the data viewer.
Chart (Hydrology)	Time-series plot comparing simulated flows from TOPMODEL, GBMM*, and VELMA* with measured flows, along with concentration of selected water-quality constituent by season. (Note: Dropdown menus allow the user to select the model flow components and water-quality constituent of interest for display.)
QW Scatter Plots	Scatter plots for measured water-quality constituents with respect to selected simulated and measured flows. (Note: A dropdown menu allows the user to select the water-quality constituent of interest for display.)
Chart (Load)	Time-series plot comparing selected simulated water-quality loads from TOPLOAD, TOPLOAD-H, LOADEST, GBMM*, and VELMA* along with measured loads. (Note: Dropdown menus allow the user to select the load model components and water-quality constituent of interest for display.)
Plot Data	Selected hydrology, water-quality, and load data are stored on this worksheet and used to generate selected plots in the data viewer.
Hydrology Data	Simulated time-series hydrologic output data from TOPMODEL, GBMM*, and VELMA* and measured flow associated with streamflow-gaging station 02175000, Edisto River near Givhans, South Carolina.
QW Data	Water-quality data for 48 water-quality constituents associated with 14 discrete measurements collected at streamflow-gaging station 02175000, Edisto River near Givhans, South Carolina.
Load Data	Simulated water-quality load data for selected water-quality constituents from TOPLOAD, TOPLOAD-H, LOADEST, GBMM*, and VELMA* along with measured loads.
Chart (TOPLOAD)	Time-series plot of simulated loads for TOPLOAD along with measured discrete loads for a selected water-quality constituent. (Note: An input table allows assignment of water-quality concentrations for the TOPLOAD computations.)
TOPLOAD	Contains TOPMODEL hydrology data and algorithms used to compute loads for TOPLOAD.
Chart (TOPLOAD-H)	Time-series plot of simulated loads for TOPLOAD-H along with measured discrete loads for a selected water-quality constituent. (Note: An input table allows assignment of water-quality concentrations for the TOPLOAD-H computations.)
TOPLOAD-H	Contains TOPMODEL and Hornberger flow component data and algorithms used to compute loads for TOPLOAD-H.
Selection Tables	Provides information used to drive selected dropdown menus and automated data retrieval in the data viewer.
Define Flow Parameters	Provides an illustration defining the surface- and subsurface-flow components associated with TOPMODEL.

*Data for GBMM and VELMA were not available at the time of report publication.

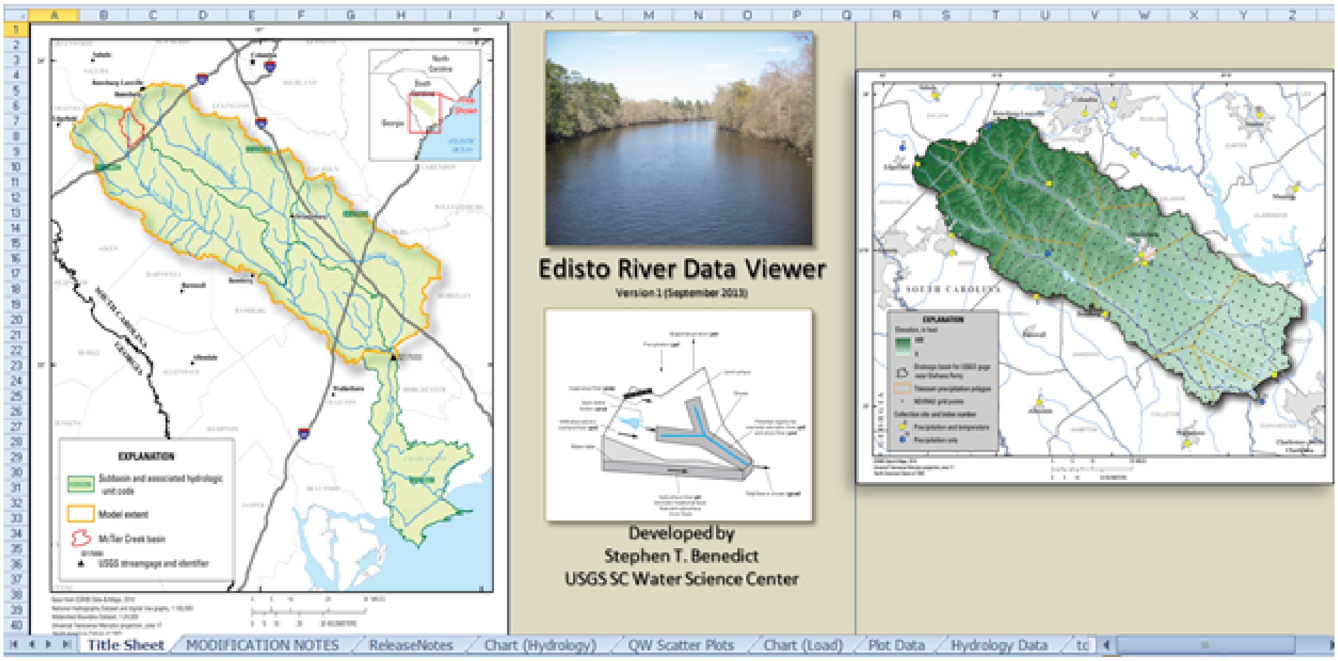

Figure 11. Screen capture from the Edisto River Data Viewer showing "Title Sheet" worksheet.

Yields are computed using the following equation:

$$Y_{Hg} = (L_{Hg}/DA) * C_y, \tag{12}$$

where

- Y_{Hg} is the mercury species (or other constituent of interest) yield, in micrograms per hectare per day;
- L_{Hg} is the mercury species (or other constituent of interest) load at the time of sampling, in milligrams per day;
- DA is the upstream watershed drainage area, in hectares; and
- C_y is a unit conversion factor (1,000).

The LOADEST program contains nine predefined regression models that can be used to estimate loads that account for the different possible combinations of explanatory variables of streamflow and time. The load equation (model 6) used in this study is as follows:

$$L = \beta_o + \beta_1 \ln Q + \beta_2 \ln Q^2 + \beta_3 \sin(2\pi T) + \beta_4 \cos(2\pi T) \tag{13}$$

where

- L is the natural logarithm (log) of the estimated load, in milligrams per day;
- β_n are the estimated coefficients for each variable;
- Q is the log of the daily mean streamflow, in cubic feet per second;
- π is pi (3.14); and
- T is the centered time, in decimal years.

For the constituent of interest, the formulated regression model was used to estimate loads over a selected time interval (estimation period), October 2004 to September 2009. All of the LOADEST model data for the Edisto River (Journey and others, 2012) were incorporated into the Edisto River Data Viewer.

TOPLOAD Results

The results of the TOPLOAD simulations for McTier Creek (Benedict and others, 2012; Golden and others, 2012) and the Edisto River are shown on figures 12 and 13, respectively. The figures include the field loads based on the measured total mercury concentrations and streamflow at the time of the field measurements, with McTier Creek having 45 field measurements during the study period and the Edisto River only having 9 measurements. Assessing the performance of the Edisto River TOPLOAD model is limited in comparison with the McTier Creek TOPLOAD model because of the limited number of Edisto River measurements; however, some similar patterns in the model performances are evident. Assuming there is a strong correlation between flow and mercury load, the TOPLOAD application can be used as a tool to evaluate which hydrologic components (flow paths) contribute to daily total mercury loading. TOPLOAD indicates that the subsurface flow component, q_{ret}, is a primary contributor to total flow, and based on the aforementioned assumption, is probably a primary contributor to the total load for both the McTier Creek and Edisto River simulations. This finding suggests that total mercury is being flushed from saturated subsurface soils, although additional investigation would be required to confirm this concept. The results for TOPLOAD–H are similar to those for TOPLOAD and, therefore, are not presented herein.

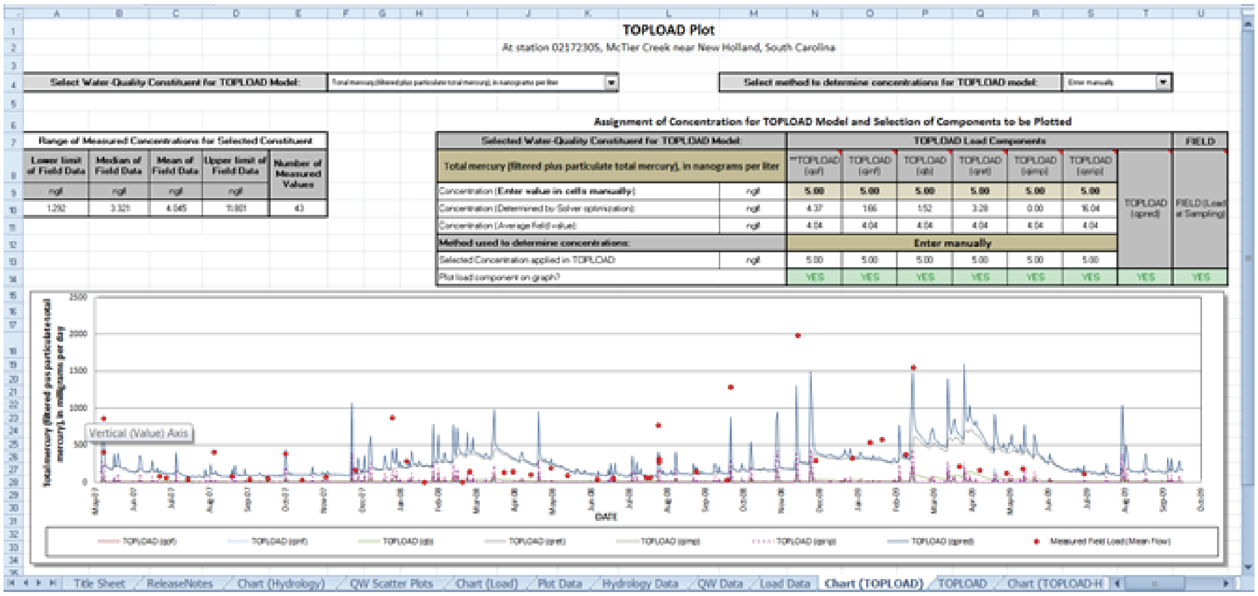

Figure 12. Screen capture from the TOPLOAD worksheet showing the simulated and measured total mercury loads for McTier Creek using manually assigned total mercury concentrations of 5 nanograms per liter for each of the TOPMODEL flow components. [Red circles indicate field loads]

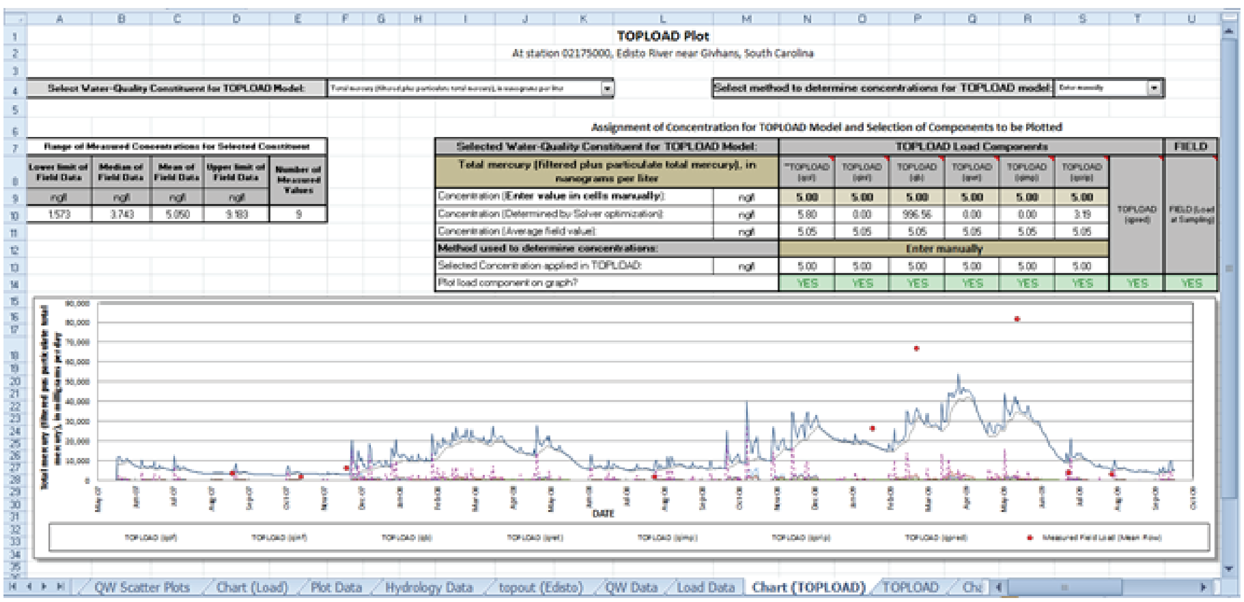

Figure 13. Screen capture from the TOPLOAD worksheet showing the simulated and measured total mercury loads for the Edisto River using manually assigned total mercury concentrations of 5 nanograms per liter for each of the TOPMODEL flow components. [Red circles indicate field loads]

Summary

As part of a larger scientific investigation to expand current understanding of linkages between hydrologic, geochemical, and ecological processes that drive fish-tissue mercury concentrations within the Edisto River, analyses and simulations of the hydrology of the Edisto River Basin were made using the topography-based hydrological model (TOPMODEL). Building on a previous application of TOPMODEL to the McTier Creek watershed, which is a small headwater catchment to the Edisto River Basin, the potential of scaling up the McTier Creek TOPMODEL to the larger Edisto River Basin was assessed using a step-wise approach. The initial TOPMODEL simulation was done using basin characteristics for the Edisto River Basin along with the calibrated parameters, meteorological data, and the topographic wetness index histogram from the McTier Creek TOPMODEL. Additional data from the Edisto River Basin were subsequently applied, and lastly, the parameter estimation program, PEST, was used to assist in calibrating model parameters for the Edisto River model. Unlike the McTier Creek TOPMODEL, which did not utilize the streamflow routing functions in TOPMODEL because of the traveltime through the system being less than the simulation time step, streamflow routing was included in the Edisto River model to account for the longer traveltimes associated with the much larger basin. The Edisto River TOPMODEL simulations were assessed using observed daily mean streamflow at U.S. Geological Survey station 0217500, Edisto River near Givhans, SC, for the period from June 13, 2007, to September 30, 2009, which was the same simulation period used at the outlet location for the McTier Creek TOPMODEL. Next-Generation Radar (NEXRAD) stage IV precipitation data were found to improve the streamflow simulations as compared to using weighted observed precipitation data from National Weather Service cooperative meteorological stations located in and around the Edisto River Basin that are part of the Global Historical Climatology Network (GHCN). It was surmised that this outcome was due to the NEXRAD rainfall data being generated from a much finer and consistent grid as compared to those used for the inverse-distance and Thiessen polygon weighting methods used with the GHCN data. The goodness-of-fit statistics for the calibrated Edisto River TOPMODEL were slightly better than those for the McTier Creek TOPMODEL, even though there is a substantial difference in the basin sizes (30.7 and 2,725 square miles, respectively). For the Edisto River model with the best goodness-of-fit statistics (simulation 7), the Nash-Sutcliffe efficiency coefficient (*NSE*) was 0.78, the Pearson's *r* was 0.89, and the percent bias (*PBIAS*) was –0.7 percent. For the McTier Creek model, the *NSE* was 0.67, *r* was 0.82, and *PBIAS* was –0.87.

Using the same digital platform developed for the McTier Creek Data Viewer, a tool developed to analyze and visualize the abundant hydrologic and water-quality data associated with the McTier Creek watershed mercury investigation, the Edisto River Data Viewer was developed for this investigation. The Edisto River Data Viewer consists of a set of Microsoft Excel spreadsheets that incorporate selected measured and modeled data at station 02175000 for the same period used in the McTier Creek investigation (June 2007 to August 2009). Applications within the Edisto River Data Viewer provide a means for visualizing selected data trends using graphs that display (1) time-series plots and scatterplots of selected hydrologic and water-quality data, (2) seasonal trends associated with selected water-quality constituents, and (3) comparison plots of selected model simulations. As was done for McTier Creek, TOPLOAD, TOPLOAD–H, and the Load Estimator (LOADEST) water-quality load models also were incorporated into the Edisto River Data Viewer. After successfully calibrating the Edisto River TOPMODEL, streamflow simulations for the Edisto River Basin were used with water-quality concentration data from McTier Creek to evaluate loads for selected water-quality constituents and the various flow components available from TOPMODEL utilizing the water-quality load models in the Edisto River Data Viewer.

References Cited

Ali, Genevieve, Oswald, C.J., Spence, C., Cammeraat, E.L.H., McGuire, K.J., Meixner, T., and Reaney, S.M., 2013, Towards a unified threshold-based hydrological theory—Necessary components and recurring challenges: Hydrological Processes v. 27, p. 313–318.

Bauch, N.J., Chasar, L.C., Scudder, B.C., Moran, P.W., Hitt, K.J., Brigham, M.E., Lutz, M.A., and Wentz, D.A., 2009, Data on mercury in water, streambed sediment, and fish tissue from selected streams across the United States, 1998–2005: U.S. Geological Survey Data Series 307, 33 p. (Also available at *http://pubs.usgs.gov/ds/307/.*)

Bedient, P.B., Huber, W.C., and Baxter, E.V., 2008, Hydrology and floodplain analysis, (4th ed): Upper Saddle River, N.J., Prentice Hall, 795 p.

Benedict, S.T., Conrads, P.A., Feaster, T.D., Journey, C.A., Golden, H.E., Knightes, C.D., Davis, G.M., and Bradley, P.M., 2012, Data visualization, time-series analysis, and mass-balance modeling of hydrologic and water-quality data for the McTier Creek watershed, South Carolina, 2007–2009: U.S. Geological Survey Open-File Report 2011–1209, 21 p. (Also available at *http://pubs.usgs.gov/of/2011/1209/.*)

Beven, K.J., 1997, Distributed hydrological modeling—Applications of the TOPMODEL concept: Chichester, England, John Wiley and Sons Ltd.

Beven, K.J., 2001, Rainfall-runoff modeling—The primer: Chichester, England, John Wiley & Sons Ltd., 360 p.

Beven, K.J., and Kirkby, M.J., 1979, A physically based, variable contributing area model of basin hydrology: Hydrological Sciences Bulletin, v. 24, p. 43–69.

Beven, K.J., and Wood, E.F., 1983, Catchment geomorphology and the dynamics of runoff contributing areas: Journal of Hydrology, v. 65, p. 139–158.

Bloom, N.S., 1992, On the chemical form of mercury in edible fish and marine invertebrate tissue. Canadian Journal of Fisheries and Aquatic Sciences v. 49, p. 1010–1017.

Bradley, P., Burns, D., Riva-Murray, K., Brigham, M., Button, D., Chasar, L., Marvin-DiPasquale, M., Lowery, M., and Journey, C.A., 2011, Spatial and seasonal variability of dissolved methylmercury in two stream basins in the eastern United States: Environmental Science and Technology v. 45, p. 2048–2055.

Bradley, P.M., Chapelle, F.H., and Journey, C.A., 2009, Comparison of methylmercury production and accumulation in sediments of the Congaree and Edisto River Basins, South Carolina, 2004–06: U.S. Geological Survey Scientific Investigations Report 2009–5021, 9 p.

Bradley, P.M., Journey, C.A., Brigham, M.E., Burns, D.A., Button, D., and Riva-Murray, K., 2013, Intra- and interbasin mercury comparisons: Importance of basin scale and time-weighted methylmercury estimates: Environmental Pollution v. 172, p. 42–52.

Bradley, P., Journey, C., Chapelle, F., Lowery, M., and Conrads, P., 2010, Flood hydrology and methylmercury availability in Coastal Plain rivers: Environmental Science & Technology v. 44, p. 9285–9290.

Bradley, P.M., Journey, C.A., Lowery, M.A., Brigham, M.E., Burns, D.A., Button, D.T., Chapelle, F.H., Lutz, M.A., Marvin-DiPasquale, M.C., and Riva-Murray, K., 2012, Shallow groundwater mercury supply in a Coastal Plain stream: Environmental Science and Technology, v. 46, p. 7503–7511.

Brigham, M.E., Wentz, D.A., Aiken, G.R., and Krabbenhoft, D.P., 2009, Mercury cycling in stream ecosystems. 1. Water column chemistry and transport: Environmental Science and Technology v. 43, p. 2720–2725.

Brumbaugh, W.G., Krabbenhoft, D.P., Helsel, D.R., Wiener, J.G., and Echols, K.R., 2001, A national pilot study of mercury contamination of aquatic ecosystems along multiple gradients: Bioaccumulation in fish: USGS/BRD/BSR—2001–0009, iii + 25 p. (Also available at *http://www.cerc.usgs.gov/pubs/center/pdfdocs/BSR2001-0009.pdf.*)

Chasar, L.C., Scudder, B.C., Stewart, A.R., Bell, A.H., and Aiken, G.R., 2009, Mercury cycling in stream ecosystems. 3. Trophic dynamics and methylmercury bioaccumulation: Environmental Science and Technology, v. 43, p. 2733–2739.

Clark, M., Rupp, D., Woods, R., Tromp-van Meerveld, H., Peters, N., and Freer, J., 2009, Consistency between hydrological models and field observations—Linking processes at the hillslope scale to hydrological responses at the watershed scale: Hydrological Processes, v. 23, p. 311–319.

Cohn, T.A., 2005, Estimating contaminant loads in rivers—An application of adjusted maximum likelihood to type 1 censored data: Water Resources Research, v. 41, W07003.

Doherty, John, 2005, PEST-Model independent parameter estimation user manual (5th ed.): Watermark Numerical Computing, 336 p.

Dunne, Thomas, and Black, R.D., 1970, Partial area contributions to storm runoff in a small New England watershed: Water Resources Research, v. 6, no. 5, p. 1296–1311.

Eidson, J.P., Lacy, C.M., Nance, Luke, Hansew, W.F., Lowery, M.A., and Hurley, N.M., Jr., 2005, Development of a 10- and 12-digit hydrologic unit code numbering system for South Carolina, 2005: U.S. Department of Agriculture, Natural Resources Conservation Service, 38 p. + 1 pl.

Esri, 2013, Create Thiessen polygons: Accessed June 10, 2013, at *http://resources.arcgis.com/en/help/main/10.1/index.html#/Create_Thiessen_Polygons/00080000001m000000/.*

Feaster, T.D., Golden, H.E., Odom, K.R., Lowery, M.A., Conrads, P.A., and Bradley, P.M., 2010, Simulation of streamflow in the McTier Creek watershed, South Carolina: U.S. Geological Survey Scientific Investigations Report 2010–5202, 61 p.

Feaster, T.D., Gotvald, A.J., and Weaver, J.C., 2009, Magnitude and frequency of rural floods in the Southeastern United States, 2006—Volume 3, South Carolina: U.S. Geological Survey Scientific Investigations Report 2009–5156, 226 p.

Feaster, T.D., Westcott, N.E., Hudson, R.J.M., Conrads, P.A., and Bradley, P.M., 2012, Comparison of TOPMODEL streamflow simulations using NEXRAD-based and measured rainfall data, McTier Creek watershed, South Carolina: U.S. Geological Survey Scientific Investigations Report 2012–5120, 33 p.

Fenneman, N.M., 1928, Physiographic divisions of the United States: Annals of the Association of American Geographers, v. 18, no. 4, p. 261–353.

Fenneman, N.M., 1938, Physiography of the eastern United States: New York, McGraw-Hill Book Co.

Fry, J., Xian, G., Jin, S., Dewitz, J., Homer, C., Yang, L., Barnes, C., Herold, N., and Wickham, J., 2011, Completion of the 2006 National Land Cover Database for the conterminous United States: Photogrammetric Engineering and Remote Sensing, v. 77, no. 9, p. 858–864.

Gesch, D., Oimoen, M., Greenlee, S., Nelson, C., Steuck, M., and Tyler, D., 2002, The National Elevation Dataset: Photogrammetric Engineering and Remote Sensing, v. 68, no. 1, p. 5–11.

Glover, J., Domino, M., Altman, K., Dillman, J., Castleberry, W., Eidson, J., and Mattocks, M., 2010, Mercury in South Carolina fishes, USA.: Ecotoxicology, v. 19, no. 4, p. 781–795.

Golden, H.E., Knightes, C.D., Conrads, P.A., Davis, G.M., Feaster, T.D., Journey, C.A., Benedict, S.T., Brigham, M.E., and Bradley, P.M., 2012, Characterizing mercury concentrations and fluxes in a Coastal Plain watershed—Insights from dynamic modeling and data: Journal of Geophysical Research, v. 117, G01006, 17 p.

Golden, H.E., Knightes, C.D., Conrads, P.A., Feaster, T.D., Davis, G.M., Benedict, S.T., and Bradley, P.M., 2013, Climate change and watershed mercury export—A multiple projection and model analysis: Environmental Toxicology and Chemistry, v. 32, no. 9, p. 2165–2174.

Grigal, D.F., 2002, Inputs and outputs of mercury from terrestrial watersheds—A review: Environmental Reviews, v. 10, no. 1, p. 1–39.

Guentzel, J.L., 2009, Wetland influences on mercury transport and bioaccumulation in South Carolina: Science of the Total Environment, v. 407, p. 1344–1353.

Helsel, D.R., and Hirsch, R.M., 1995, Statistical methods in water resources: Amsterdam, Elsevier Science, Studies in Environmental Science, v. 49, 529 p.

Hornberger, G.M., Bencala, K.E., and McKnight, D.M., 1994, Hydrological controls on dissolved organic carbon during snowmelt in the Snake River near Montezuma, Colorado: Biogeochemistry, v. 25, p. 147–165.

Hornberger, G.M., Beven, K.J., Cosby, B.J., and Sappington, D.E., 1985, Shenandoah watershed study—Calibration of a topography-based, variable contributing area hydrological model to a small forested catchment: Water Resources Research, v. 21, p. 1841–1850.

Hornberger, G.M., Raffensperger, J.P., Wiberg, P.L., and Eshleman, K.N., 1998, Elements of physical hydrology: Baltimore, Md., The John Hopkins University Press.

Inamdar, Shreeram, 2009, Course notes from Bioresources Engineering 622: University of Delaware, accessed September 24, 2009, at *http://udel.edu/~inamdar/BREG622/TOPIndex.pdf*.

Janssen, P.H.M., and Heuberger, P.S.C., 1993, Calibration of process-oriented models: Ecological Modelling, v. 83, p. 55–66.

Journey, C.A., Burns, D.A., Riva-Murray, Karen, Brigham, M.E., Button, D.T., Feaster, T.D., Petkewich, M.D., and Bradley, P.M., 2012, Fluvial transport of mercury, organic carbon, suspended sediment, and selected major ions in contrasting stream basins in South Carolina and New York, October 2004 to September 2009: U.S. Geological Survey Scientific Investigations Report 2012–5173, 125 p.

Junk, W.J., Bayley, P.B., Sparks, R., 1989, The flood pulse concept in river-floodplain systems: Canadian Special Publication of Fisheries and Aquatic Science v. 106, p. 110–127.

Kennen, J.G., Kauffman, L.J., Ayers, M.A., Wolock, D.M., and Colarullo, S.J., 2008, Use of an integrated flow model to estimate ecologically relevant hydrologic characteristics at stream biomonitoring sites: Ecological Modelling, v. 211, p. 57–76.

Krabbenhoft, D.P., Wiener, J.G., Brumbaugh, W.G., Olson, M.L., DeWild, J.F., and Sabin, T.J., 1999, A national pilot study of mercury contamination of aquatic ecosystems along multiple gradients, *in* U.S. Geological Survey Toxic Substances Hydrology Program—Proceedings of the Technical Meeting Charleston, South Carolina, March 8–12, 1999, Volume 2 of 3—Contamination of hydrologic systems and related ecosystems: U.S. Geological Survey Water-Resources Investigations Report 99–4018B, p. 147–160. (Also available at *http://toxics.usgs.gov/pubs/wri99-4018/Volume2/sectionB/2301_Krabbenhoft/pdf/2301_Krabbenhoft.pdf*.)

Krause, P., Boyle, D.P., and Bäse, F., 2005, Comparison of different efficiency criteria for hydrological model assessment: Advances in Geosciences, v. 5, p. 89–97.

Legates, D.R., and McCabe, G.J., Jr., 1999, Evaluating the use of "goodness-of-fit" measures in hydrologic and hydroclimatic model validation: Water Resources Research, v. 35, no. 1, p. 233–241.

Lorenz, D.L., and others, 2011, USGS library for S–PLUS for Windows—Release 4.0: U.S. Geological Survey Open-File Report 2011–1130.

Marshall, W.D., ed., 1993, Assessing change in the Edisto River Basin—An ecological characterization: South Carolina Water Resources Commission Report no. 177, 149 p.

Marvin-DiPasquale, M., Lutz, M.A., Brigham, M.E., Krabbenhoft, D.P., Aiken, G.R., Orem, W.H., Hall, B.D., 2009, Mercury cycling in stream ecosystems. 2. Benthic methylmercury production and bed sediment-pore water partitioning: Environmental Science and Technology, v. 43, p. 2726–2732.

Menne, M.J., Durre, Imke, Vose, R.S., Gleason, B.E., and Houston, T.G., 2012, An overview of the Global Historical Climatology Network–Daily database: Journal of Atmospheric and Oceanic Technology, v. 29, p. 897–910.

Mergler, D., Anderson, H.A., Chan, L.H.M., Mahaffey, K.R., Murray, M., Sakamoto, M., Stern, A.H., 2007, Methylmercury exposure and health effects in humans—A worldwide concern: Ambio, v. 36, p. 3–11.

Moriasi, D.N., Arnold, J.G., Van Liew, M.W., Bingner, R.L., Harmel, R.D., and Veith, T.L., 2007, Model evaluation guidelines for systematic quantification of accuracy in watershed simulations: Transactions of the American Society of Agricultural and Biological Engineers, v. 50, no. 3, p. 885–900.

Nash, J.E., and Sutcliffe, J.V., 1970, River flow forecasting through conceptual models—Part I. A discussion of principles: Journal of Hydrology, v. 10, p. 282–290.

National Oceanic Atmospheric Administration, 2013, NOAA's weather and climate toolkit: Accessed June 3, 2013, at *http://www.ncdc.noaa.gov/oa/wct/batch.php*.

National Weather Service, 2013, The hydrometeorological automated data system: Accessed June 3, 2013, at *http://www.nws.noaa.gov/oh/hads/WhatisHADS.html*.

Natural Resources Conservation Service, 2008, Soil survey geographic database: Accessed June 8, 2008, at *http://www.soils.usda.gov/survey/geography/ssurgo/*.

Natural Resources Conservation Service, 2013, Soil data viewer: Accessed April 6, 2013, at *http://soils.usda.gov/sdv/*.

Norman, G.R., and Streiner, D.L., 1997, PDQ statistics: St. Louis, Mo., Mosby-Year Book, Inc., 188 p.

Nystrom, E.A., and Burns, D.A., 2011, TOPMODEL simulations of streamflow and depth to water table in Fishing Brook Watershed, New York, 2007–09: U.S. Geological Survey Scientific Investigations Report 2011–5190, 54 p.

Quinn, P.F., Beven, K.J., and Lamb, R., 1997, the ln(a/tanβ) index—How to calculate it an how to use it within the TOPMODEL framework, *in* Beven, K.J., ed., Distributed hydrological modeling—Applications of the TOPMODEL concept: Chichester, England, Wiley, p. 31–52.

Runkel, R.L., Crawford, C.G., and Cohn, T.A., 2004, Load Estimator (LOADEST): A FORTRAN program for estimating constituent loads in streams and rivers: U.S. Geological Survey Techniques and Methods, book 4, chap. A5, 69 p.

St. Louis, V.L., Rudd, J.W., Kelly, C., Beaty, K.G., Bloom, N.S., and Flett, R.J., 1994, Importance of wetlands as sources of methyl mercury to boreal forest ecosystems: Canadian Journal of Fisheries and Aquatic Sciences, v. 51, p. 1065–1076.

Sauer, V.B., and Turnipseed, D.P., 2010, Stage measurement at gaging stations: U.S. Geological Survey Techniques and Methods, book 3, chap. A7, 45 p.

Scheuhammer, A.M., Basu, N., Evers, D.C., Heinz, G.H., Sandheinrich, M.B., and Bank, M.S., 2012, Ecotoxicology of mercury in fish and wildlife—Recent advances, *in* Bank, M.S., ed., Mercury in the environment—Pattern and process: Berkeley, Calif., University of California Press.

Scheuhammer, A.M., Meyer, M.W., Sandheinrich, M.B., and Murray, M.W., 2007, Effects of environmental methylmercury on the health of wild birds, mammals, and fish: AMBIO—A Journal of the Human Environment, v. 36, p. 12–19.

Scudder, B.C., Chasar, L.C., Wentz, D.A., Bauch, N.J., Brigham, M.E., Moran, P.W., and Krabbenhoft, D.P., 2009, Mercury in fish, bed sediment, and water from streams across the United States, 1998–2005: U.S. Geological Survey Scientific Investigations Report 2009–5109, 74 p. (Also available at *http://pubs.usgs.gov/sir/2009/5109.*)

Searcy, J.K., 1959, Flow-duration curves, manual of hydrology—Part 2. Low-flow techniques: U.S. Geological Survey Water-Supply Paper 1542–A, 33 p.

Sedell, J.R., Richey, J.E., and Swanson, F.J., 1989, The river continuum concept—A basis for the expected ecosystem behavior of very large rivers?: Canadian Special Publication of Fisheries and Aquatic Science v. 106, p. 49–55.

Singh, V.P., 1995, Computer models of watershed hydrology: Highlands Ranch, Colo., Water Resources Publications.

Sivapalan, M., 2003, Process complexity at hillslope scale, process simplicity at the watershed scale—Is there a connection?: Hydrological Processes, v. 17, p. 1037–1041. South Carolina Department of Health and Environmental Control, 2012, Watershed water quality assessment—Edisto River Basin: Columbia, S.C., Bureau of Water Technical Report no. 103J–12.

South Carolina Department of Natural Resources, 2009, South Carolina State Water Assessment (2d ed): Land, Water & Conservation Division, 407 p.

Thorp, J.H., Thoms, M.C., and DeLong, M.D., 2006, The riverine ecosystem synthesis—Biocomplexity in river networks across space and time: River Research and Applications, v. 22, p. 123–147.

U.S. Environmental Protection Agency, 2011, 2010 Biennial national listing of fish advisories: Washington, D.C., U.S. Environmental Protection Agency, Office of Water, EPA–820–F–11–014.

U.S. Environmental Protection Agency, 2013, Total maximum daily loads (TMDLs) and mercury: U.S. Environmental Protection Agency Web page accessed October 31, 2013, at *http://water.epa.gov/lawsregs/lawsguidance/cwa/tmdl/mercury/index.cfm*.

U.S. Geological Survey, 2007, Facing tomorrow's challenges—U.S. Geological Survey science in the decade 2007–2017: U.S. Geological Survey Circular 1309. (Also available at *http:// pubs.er.usgs.gov/usgspubs/cir/cir1309*.)

U.S. Geological Survey, 2012, Water-resources data for the United States for water year 2012: U.S. Geological Survey Water-Data Report WDR–US–2012, site 02175000, accessed August 2013 at *http://wdr.water.usgs.gov/wy2012/pdfs/02175000.2012.pdf*.

Vannote, R.L., Minshall, G.W., Cummins, K.W., Sedell, J.R., and Cushing, C.E., 1980, The river continuum concept: Canadian Journal of Fisheries and Aquatic Science, v. 37, p. 130–137.

Vigil, J.F., Pike, R.J.; and Howell, D.G., 2000, A tapestry of time and terrain: U.S. Geological Survey Geologic Investigations Series 2720, 1 plate, 1:2,500,000, 1 pamphlet. (Also available at *http://pubs.usgs.gov/imap/i2720/*.)

Ward, D., Nislow, K., and Folt, C., 2010, Bioaccumulation syndrome: identifying factors that make some stream food webs prone to elevated mercury bioaccumulation: Annals of the New York Academy of Sciences, v. 1195, p. 62–83.

Whipkey, R.Z., 1965, Subsurface stormflow from forested slopes: Hydrological Sciences Bulletin, v. 10, p. 74–85.

Williamson, T.N., Odom, K.R., Newson, J.K., Downs, A.C., Nelson H.L., Jr., Cinotto, P.J., and Ayers, M.A., 2009, The Water Availability Tool for Environmental Resources (WATER)—A water-budget modeling approach for managing water-supply resources in Kentucky—Phase I—Data processing, model development, and application to non-karst areas: U.S. Geological Survey Scientific Investigations Report 2009–5248, 34 p.

Wolock, D.M., 1993, Simulating the variable-source-area concept of streamflow generation with the watershed model TOPMODEL: U.S. Geological Survey Water-Resources Investigations Report 93–4124, 33 p.

For further information about this publication contact:

Director
U.S. Geological Survey
South Carolina Water Science Center
Stephenson Center, Suite 129
720 Gracern Road
Columbia, SC 29210–7651

Or visit the South Carolina Water Science Center Web site at
http://sc.water.usgs.gov/

Prepared by the Raleigh Publishing Service Center

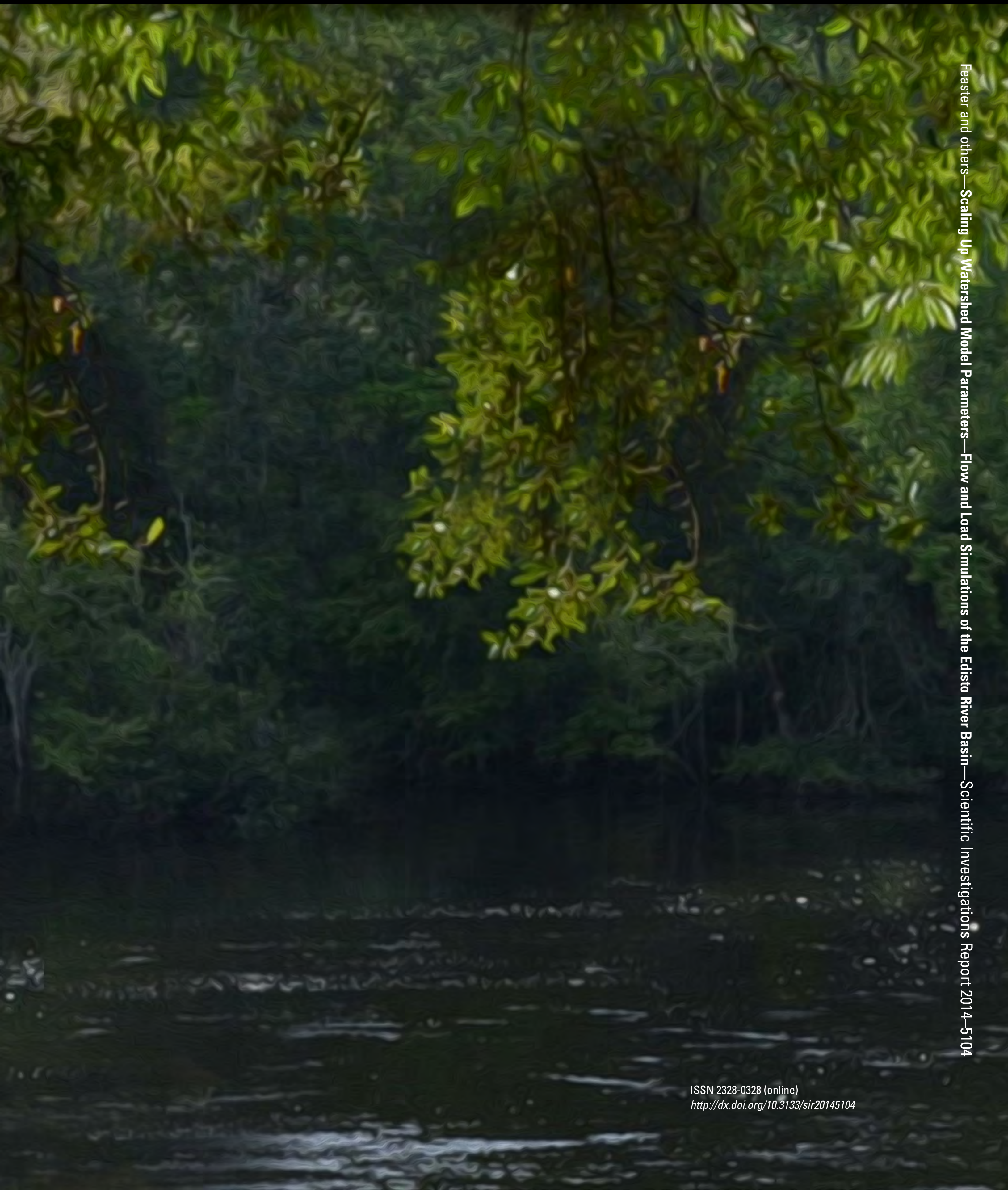

Feaster and others—**Scaling Up Watershed Model Parameters—Flow and Load Simulations of the Edisto River Basin**—Scientific Investigations Report 2014–5104

ISSN 2328-0328 (online)
http://dx.doi.org/10.3133/sir20145104